Arno thought we would like to review these papers on the foundations for tying in stability analyses and transition

Jerry Lee

From K. Stetson
2003

SMITH 1956

TRANSITION, PRESSURE GRADIENT AND STABILITY THEORY

by

A. M. O. Smith and Nathalie Gamberoni

Report No. ES 26388

August 31, 1956

DOUGLAS AIRCRAFT DIVISION

TRANSITION, PRESSURE GRADIENT AND STABILITY THEORY

by

A. M. O. Smith and Nathalie Gamberoni

Report No. ES 26388 August 31, 1956

DOUGLAS AIRCRAFT COMPANY, INC.

EL SEGUNDO DIVISION

Engineering DEPARTMENT

REPORT NUMBER

ES 26388

TRANSITION, PRESSURE GRADIENT, AND STABILITY THEORY

CONTRACT NO. None

REPORT DATE August 31, 1956

MODEL None

CLASSIFICATION None

PREPARED BY Aerodynamics Research*

SECTION OR GROUP Aerodynamics

APPROVED BY K. E. Von Ezra
Chief, Aerodynamics Section

APPROVED BY

* A. M. O. Smith
Nathalie Gamberoni

REVISIONS

LETTER	DATE	PAGES AFFECTED	REMARKS

DOUGLAS AIRCRAFT COMPANY, INC. EL SEGUNDO DIVISION EL SEGUNDO, CALIFORNIA

ABSTRACT

This article presents a method of predicting transition that is founded upon the theory of boundary-layer stability. It considers both plane and axially symmetric flows of a very low-turbulence incompressible stream past very smooth bodies.

According to stability theory, self-energized disturbances form in the boundary layer and slowly grow in strength while moving downstream, until they ultimately cause the boundary layer to become turbulent, by a process as yet unknown. J. Pretsch has computed a family of charts by means of which the apparent growth of these waves can be calculated so that correlation with experiment becomes possible.

The theory and its implications are reviewed and discussed. Nearly all the applicable experimental transition data have been studied and correlated with the calculations made with the aid of Pretsch's charts. A strong correlation of experimental results with this theory was discovered. In fact, to first order, Tollmien-Schlichting waves were found to undergo an apparent amplification ratio $\exp\int \beta_i \, dt$ equal to about e^9 by the time transition began. This value was then used to predict transition for a considerable variety of flows, both in wind tunnels and in flight. The predictions agree quite well with experiment, particularly in view of the nature of the experimental data.

In contrast, R_{δ^*} or R_θ at the beginning of transition vary greatly with pressure gradient and are not at all suitable alone as fundamental guides for locating transition. As a measure of transition on bodies of revolution R_{δ^*} is even less satisfactory than it is for two-dimensional flows. However, the method based on stability theory correlates both types of flow with equal accuracy.

A short-cut empirical method of predicting transition, due to Michel, has been studied. In two dimensional flow its validity was found to be good, and the reason for its success can be explained by stability theory.

NOTATION

a	amplification ratio, that is, the ratio of the amplitude of a disturbance in the boundary layer to its amplitude at the point of neutral stability; a function of R_{δ^*}
b	a constant in Eq. (1)
c	wing chord or other characteristic reference length
c_{f_L}	local laminar-skin-friction coefficient
c_r	phase velocity of propagation of Tollmien-Schlichting waves
k	correlation coefficient, $\overline{uv}/u'v'$
R_c	Reynolds number based on chord, $U_\infty c/\nu$
R_x	x-Reynolds number, Ux/ν
R_{δ^*}	boundary-layer Reynolds number based on displacement thickness, $U\delta^*/\nu$
R_θ	boundary-layer Reynolds number based on momentum thickness, $U\theta/\nu$
t	time
u	instantaneous velocity in the boundary layer in the x-direction
u'	root-mean-square value of velocity fluctuations in the x-direction
U	local mean velocity at edge of the boundary layer in the x-direction
U_∞	reference velocity, usually the free-stream velocity
v	instantaneous velocity in the boundary layer in the y-direction
v'	root-mean-square value of velocity fluctuations in the y-direction
w	instantaneous velocity in the boundary layer in the z-direction
x	distance along the surface of the body measured from the upstream stagnation point
X	distance along the chord or axis of the body
y	distance perpendicular to the surface of the body
α	2π divided by the wave length λ of the disturbance

β	Hartree's beta defined by $U \backsim x^{\beta/(2-\beta)}$
β_i	amplification coefficient, where $\exp \int_{t_n}^{t} \beta_i \, dt \equiv a$, the amplification ratio
β_r	oscillation frequency measured in radians per second
δ^*	displacement thickness of the boundary layer
θ	momentum thickness of the boundary layer
λ	wave length of the disturbance
λ_P	Pohlhausen's lambda, $(\delta^2/\nu)\, dU/dx$
μ	dynamic viscosity
ν	kinematic viscosity
ρ	mass density
τ_A	apparent shear stress caused by the disturbances in the boundary layer, $-\rho\overline{uv}$
τ_L	mean laminar shear stress, $\mu\, \partial\bar{u}/\partial y$, where $\bar{u}$ is the mean velocity

SUBSCRIPTS

n	where Tollmien-Schlichting waves first become unstable, the neutral point
tr	beginning of the transition region

INTRODUCTION

This article reports on efforts to verify or disprove one theory of the transition process in the restricted case of incompressible flow with arbitrary pressure distribution over a very smooth, convex surface in a stream of very low turbulence. Both two-dimensional and axially symmetric flows are examined. The theory being investigated is that disturbances

in the boundary layer grow at the rate predicted by solutions of the Orr-Sommerfeld equation, growth continuing until transition occurs.

The calculation methods and charts available for verification or disproof of the hypothesis are most unsatisfactory. Indeed if the methods and charts were slightly worse, no check would be possible at all. Furthermore, available experimental data are poor and full of scatter. But, as well as can be ascertained from the combination of inaccurate data and inadequate computing methods, the experimental effect of pressure gradient on transition and predictions by the subject theory are in good agreement.

Before details of the investigation are given, a brief review of past theories and work on the problem will be made, in order to provide proper orientation for what follows.

Early Research

In 1937 when B. Melvill Jones presented the first Wright Brothers Lecture (Ref. 1), the phenomenon of transition was almost a complete mystery; except in a few special flow situations, hardly any factual data were available. For this very reason Jones' lecture, which presented flight measurements on transition, added so much to the store of knowledge that it strongly influenced subsequent aerodynamic research. In this period, experimental work was carried on under severe handicaps. Tunnel turbulence was high; hot-wire equipment was not nearly so advanced, particularly the auxiliary equipment; and transition was so difficult to detect that adequate data were most rare.

In the realm of theory, two schools of thought existed, that of G. I. Taylor and that of the Göttingen group under Prandtl. Taylor hypothesized that transition was set off by a small region of reverse flow in the boundary layer, imposed by turbulence in the main stream (Ref. 2). His analysis enjoyed a partial success, for it proved capable of predicting the effect of turbulence on the critical Reynolds number of a sphere in the high-turbulence tunnels of two or three decades ago. The reverse-flow concept of his theory implies that transition will occur only when some boundary-layer Reynolds number such as $R_{\delta*}$ is exceeded. The theory has little to do with the history of the boundary layer except as it affects $R_{\delta*}$. An obvious deduction from his hypothesis is, of course, that if the turbulence approaches zero, the laminar run $R_{x_{tr}}$

will approach infinity, provided no separation exists in the steady or ordinary sense.

Taylor's theory was investigated further by Hall and Hislop (Ref. 3) for flat plates and by Fage and Preston (Ref. 4) for bodies of revolution. The phenomenon conceived and analyzed by Taylor was shown to exist for these different bodies also, but results failed to show that a method for predicting transition could be founded on the phenomenon alone, particularly if pressure gradients exist. Later work in streams of lower turbulence showed that Taylor's phenomenon loses its dominance, that is, although it is significant in flows of high turbulence, it is not a determining factor in those of low turbulence. Finally, his theory is quite unable to account for the known difference in $R_{\theta_{tr}}$ or $R_{\delta^*_{tr}}$ occurring on bodies of revolution and two-dimensional shapes.

The Göttingen group, especially Tollmien and Schlichting (Ref. 5), advanced the hypothesis that small disturbances become unstable at some x-location in the boundary layer and gradually grow in strength until the amplitude is sufficient to cause transition. The theory made no attempt to describe the final part of the process but it did present an explanation of the start of the entire sequence of developments. This second approach takes account of the boundary layer development in far more detail; it not only considers the evolution of R_θ or R_{δ^*} but also it considers the complete history of the stability of the boundary layer. Unfortunately, at that time instrumentation was inadequate and wind tunnels were too turbulent to detect the type of wave motion predicted by the elegant theoretical calculations. The only experimental evidence supporting its existence was supplied by a divergent channel, a low-speed wake and an accoustically sensitive jet.

In view of the two conflicting theories, one almost completely unsubstantiated, the other somewhat substantiated but hardly applicable to flight conditions, the best Jones could do was to state that transition must be related to R_{δ^*}. His effort at correlating measured transition points in terms of $R_{\delta^*_{tr}}$ and $\lambda_{P_{tr}}$ was quite unsuccessful. Because no simple relation between a transition parameter and a pressure-gradient parameter could be found, transition

was commonly estimated by assuming a value of R_{δ^*} at transition, but there was no method of changing its value as the pressure distribution changed. It was known that accelerating velocities favored laminar flow, but that was all, for no theoretical or experimental method was available to predict a variation of $R_{\delta^*_{tr}}$. The method of selecting a boundary-layer Reynolds number as a criterion goes back at least to Gruschwitz (Ref. 6), who proposed that $R_\theta = 600$ be used as the transition criterion.

In short, the method for estimating transition in current use may be stated as follows:

Using past knowledge and test experience, select an allowable value of R_{δ^*}, say about 3000 if for free flight. Then for the value of R_c and lift coefficient under consideration calculate the growth of R_{δ^*} as a function of the distance from the forward stagnation point. Transition should occur where the allowable value of R_{δ^*} is first exceeded.

No rational hypothesis was available to account for changes in pressure distribution.

Recent Developments

About 1940 Schubauer and Skramstad (Ref. 7) began investigating the effect of turbulence on the location of transition on a flat plate. In the process of reducing the turbulence to very low values they made the important discovery that the waves calculated by Tollmien and Schlichting could now be found in the boundary layer. Apparently the high level of turbulence in other wind tunnels had always camouflaged the signal. The experiments of these investigators fully confirmed Schlichting's calculations and of course finally proved the existence of these waves.

Of course, in flight turbulence is low and therefore the work of Schubauer and Skramstad should be applicable. Yet many questions remained unanswered concerning the applicability of stability theory to other more general flows and to the complete transition process. For example, only a small degree of tunnel turbulence was found to obscure the waves completely. Furthermore, the theory assumes zero turbulence and a mathematically smooth wall, that is, no external excitation of the waves comes from either side of the boundary layer.

In 1951 Emmons formally advanced and analyzed an idea that had been suspected

for some time (Ref. 8 and 9). He showed that the actual transition region begins with local ''spots'' of turbulent flow. These spots grow, spread, and coalesce until uniform turbulent flow is developed, marking the end of the transition region. Emmons noticed the spots in a shallow water-channel flow. Since then, the same type has been observed and studied in air flow.(Ref. 10).

Although his deductions are valid and the theory accounts for the effect of turbulence better than Taylor's, Emmons' analysis does not consider how the transition process starts, but only what happens once it starts. Hence, although it contributes significantly to the understanding of the total process, it sheds no light on the effect of the velocity distribution upon the location of transition. In fact, Emmons' analysis begins with an assumed turbulent spot production and distribution function $g(x, y, t)$ and proceeds from there. But before the transition point can be predicted, the g-function must be predicted. In a way the analysis of this report sheds light on the nature of the g-function.

In flows of very low turbulence the influence of Tollmien-Schlichting waves was understood and accepted. But does this type of wave motion have any bearing on the transition process in flows of low to medium turbulence? The answer is in the affirmative. Bennett (Ref. 11), using high-quality hot-wire and frequency-spectrum instrumentation, detected a strong influence of the Tollmien-Schlichting wave growth in the boundary-layer flow on a flat plate in a tunnel whose turbulence level was as high as $u'/U_\infty = 0.42$ percent. Bennett's frequency-spectra measurements showed that the frequency receiving the greatest amplification was substantially that predicted by stability theory. Originally Schubauer and Skramstad discovered the waves only after the turbulence had been reduced to about 0.05 percent.

Bennett's work supplies further evidence that the Tollmien-Schlichting wave phenomenon influences the transition process. But next we shall introduce a note of confusion. Stability theory deals with two-dimensional waves. Recently in personal discussions with F. X. Wortmann, the writer learned about his experiments at the Institut für Gasströmungen der Technischen Hochschule, Stuttgart. Wortmann has been using the tellurium-wire technique (Ref. 12) to study Tollmien-Schlichting waves in water in a two-dimensional channel. Much

as he tried, he could never create a two-dimensional wave, for a w-component always existed. Schubauer and Skramstad also noticed in their tests that the flow had a w-component. Wortmann's work is reported in ''50 Jahre Grenzschichtforschung'' (Ref. 13).

In February, 1956 Laufer (Ref. 14) detected the same type of oscillations in a supersonic boundary layer at a Mach number of 2.15.

In 1951 Michel (Ref. 15) produced the first method-known to the writer-of predicting the transition point that could take the pressure gradient into account. Michel plotted $R_{\theta_{tr}}$ versus $R_{x_{tr}}$ from available test data and obtained a well defined single curve, and so, for the first time a general method became available. It was strictly empirical but it did supply reasonable answers. Later in this paper his method is treated at greater length.

Factors Involved in the Transition Process

The current state of knowledge concerning transition has been ably summarized in Dryden's comprehensive report (Ref. 16). However, for clarity the situation will be reviewed briefly. Transition appears to be influenced by the following factors at least:

a. Free-stream turbulence
b. Pressure gradient
c. Surface curvature
d. Roughness
e. Noise and vibration
f. Surface temperature
g. Mach number
h. Secondary flow effects-sweep, etc.

Taylor's theory is unsatisfactory for flows of low turbulence. Liepmann (Ref. 17) has shown that curvature influences transition only when the wall is concave. As roughness, noise, surface temperature, Mach number and secondary-flow effects are beyond the scope of this article, and as most surfaces of interest are convex, we shall confine our attention to the effect of pressure gradient on a flow over a smooth, convex surface. The turbulence

problem will be avoided by assuming the flow to be of low turbulence-technically the most important case, since it is the type occurring in free flight.

Current Concept of Transition

Before restricting ourselves to the effect of pressure gradient, we shall state explicitly the current speculative concept of the transition process in two-dimensional or axially symmetric flows of low turbulence. It is as follows:

a) The initial boundary-layer flow is stable to Tollmien-Schlichting waves, but nevertheless it is agitated by disturbances impressed upon it by external turbulence, surface roughness, noise, and vibration.

b) At some point on the surface the flow becomes unstable and Tollmien-Schlichting waves begin to grow. On a perfect surface in a flow of zero turbulence, without noise or vibration, the disturbance will continue to grow, solely because of the self-excited nature of the wave. But in an actual flow the disturbances will be further excited by surface roughness and vibration as well as by external turbulence and noise. Thus the true flow is similar to a forced vibration. The writer likes to think of a homely analogy that describes the flow. It may be compared to an automobile running along a rough road in a gusty wind. The engine vibrations correspond to Tollmien-Schlichting waves, the bumpy road corresponds to the imperfect surface, and the gusty weather corresponds to the external turbulence. The motion of the automobile, like the motion within the boundary layer, is the response to all three factors.

c) The disturbances grow in strength until they suddenly break over into spots of turbulence. There is no reason to expect the break-over process to be two-dimensional, for two reasons: first, at the beginning of amplification the disturbances receiving amplification are random in both strength and location, and second, even though Tollmien-Schlichting waves enter into the amplification process, the waves do not show much evidence of two-dimensionality. In other words, the wave phenomenon exists in the small rather than in the large.

d) These spots of turbulence are washed downstream and grow in all directions and coalesce until finally the flow is entirely turbulent.

Statements (c) and (d) imply that transition occurs over a region, not at a point. But for convenience and in deference to custom, the term transition point will continue to be used. In this article, it normally means the point where transition begins.

THE PROBLEM UNDER INVESTIGATION

At the present state of the art no theoretical procedure is available that can potentially account for all the effects mentioned in the speculative theory of transition. Stability theory takes account only of self-excitation of waves in the boundary layer, and since it is the only theory available, correlation studies must be confined to smooth surfaces in tunnels of very low turbulence. Therefore our problem is the following important but restricted one.

Can stability theory be used to provide a method for predicting the beginning of transition in an arbitrary incompressible flow over a very smooth convex or flat surface in a stream of very low turbulence, with the further restriction that the flow be either two-dimensional or axially symmetric?

Details of the Theory and Calculation Procedure

Liepmann (Ref. 17) has enunicated a logical basis for the application of the theory that appears sound, regardless of the final mechanism of the breakdown of the laminar flow. He makes the following statement about $R_{x_{tr}}$, the x-Reynolds number for transition:

''$R_{x_{tr}}$ is the Reynolds number at which the apparent shear $\tau_A = -\rho\overline{uv}$ due to amplified boundary-layer oscillations at any point in the boundary layer becomes equal to the laminar shear $\tau_L = \mu\,\partial u/\partial y$ in the boundary layer''.

R_{x_n} represents the point for neutral stability, and since $R_{x_{tr}}$ is usually reached far downstream of R_{x_n}, application of Liepmann's hypothesis requires calculation of the amplitude of the disturbances. Liepmann derives an approximate formula for application of the above principle that incorporates a

quantity calculable by stability theory. It is:

$$\frac{\tau_{A_{max}}}{\tau_L} \approx -\frac{2}{c_{f_L}} \left\{ kb\left(\frac{u'}{U}\right)^2 \left[a(R_{\delta^*})\right]^2 \right\}_{max} \qquad (1)$$

In this expression:

$\tau_{A_{max}}$ = $-\rho\overline{uv}_{max}$, the maximum value of the apparent shear stress caused by the disturbances

τ_L = $\mu\, \partial\bar{u}/\partial y$, the laminar shear stress

c_{f_L} = the local laminar-skin-friction coefficient at any point x

b = factor of proportionality such that $v'/U = b(u'/U)$

k = $\overline{uv}/u'v'$, the correlation coefficient

$(u'/U)_n$ = the turbulent fluctuation level at the beginning of instability (neutral point)

$a(R_{\delta^*})$ = the amplification ratio

When $\tau_{A_{max}}/\tau_L \approx 1$, transition should occur. Hence Eq. (1) states that transition will be affected by the local skin-friction coefficient, the turbulence structure of the stream, and the amplification factor.

The Pretsch Charts

The preceding discussion makes no assumption that the disturbance is a Tollmien-Schlichting wave, but if it is, it becomes possible to compute the amplification factor by means of Pretsch's charts.(Ref. 18 and 19). Pretsch computed the amplification rate of Tollmien-Schlichting waves for several of the two-dimensional-wedge flows, namely, those with Hartree $\beta = -0.198$, -0.10, 0, 0.2, 0.6, and 1.0. Two types were computed, rate charts showing the rate of growth of disturbances of various frequencies and cumulative amplification charts for constant-β flows, showing the total amplification up to any value of R_{δ^*}. Pretsch (Ref. 19 and 20) has shown that for boundary-layer flows in a stream of non-constant velocity the basic analysis is valid whether they be two-dimensional or axially symmetric.

Fig. 1 presents the family of neutral-stability curves derived from those computed by Pretsch. Some of the curves were obtained by interpolation between

those of his original set. Fig. 2 presents the set of amplification rate charts prepared from his work. They have been constructed by careful cross-fairing of his original smaller set and are plotted on ordinary semi-log graph paper to facilitate their use. Pretsch's charts of amplification ratio included in Ref. 19 are not necessary, as will be seen later, and so are not included herein. The rate charts of Fig. 2 are applicable to both plane and axially symmetric flow.

If the frequency β_r of a certain wave, the boundary-layer Reynolds number, and Hartree's β are known, the rate of amplification β_i can be read from the charts. Therefore, during a time interval (t_1, t_2) a particular frequency will undergo an amplification of amount

$$a(R_{\delta^*}) = \exp \int_{t_1}^{t_2} \beta_i \, dt \qquad (2)$$

By now the procedure indicated by Eq. (1) should be clear. In determining the value of $\tau_{A_{max}} / \tau_L$ at some point on a surface, one seeks the frequency that will produce the highest value of the subject quantity. The highest value of the product $k(u'/U)_n \left[a(R_{\delta^*})\right]$ is being sought not the highest value of $a(R_{\delta^*})$ alone. Therefore a careful evaluation of Eq. (1) demands at least a frequency spectrum to supply data on initial values of the disturbance. A mean value of u'/U is unsatisfactory, for the highest value of $a(R_{\delta^*})$ may occur at some frequency for which u'/U is low, but at some other frequency u'/U may be enough greater to produce a larger value of the product $k(u'/U) \left[a(R_{\delta^*})\right]$, even though $a(R_{\delta^*})$ is below the maximum. In short, the product should be maximized, theoretically.

The above philosophy is accepted, but in the following correlation studies it can be applied only partially. First of all, a knowledge of the spectrum of the turbulence is not available. In some cases an over-all average value of u'/U is available, but, as has just been explained, it is insufficient. Furthermore, it is not clear that the magnitude of disturbances at the neutral point is directly proportional to the free-stream turbulence. Finally, except near separation, c_{f_L} changes little with types of flow. For example,

in constant-β types of flow (Ref. 21),

$$c_{f_L} = \frac{2}{R_{\delta^*}} \Delta^* F''(0) \qquad (3)$$

For $\beta = 0$, $2\Delta^* F''(0) = 1.143$, and for $\beta = 1$, $2\Delta^* F''(0) = 1.597$. Therefore except near separation c_{f_L} is nearly independent of β -it is a minor variable-while $a(R_{\delta^*})$ is found from experimental data to be the major variable-of the order of e^9 (= 8103). Then in any first-order correlation study, variations of all factors except $a(R_{\delta^*})$ can be neglected.

Method for Correlation with Experimental Data

Assuming the flow is not of a constant-β type, the ideal procedure for analyzing experimental results would require: (a) accurate calculation of boundary-layer profiles along the entire given flow; (b) for these specific profiles, calculation of rate charts similar to those of Fig. 2; (c) use of these charts for computation of the highest amplification factor.

Since such would be a colossal undertaking, the growth of disturbances was computed in a much cruder fashion designed to use Pretsch's charts, Fig. 2. His charts require knowledge of R_{δ^*} and β. These two required properties have been computed by the method of Ref. 22, a rapid method that uses β as a parameter and has a high degree of accuracy for most accelerating flows.

According to stability theory, disturbances will grow as $\exp \int \beta_i \, dt$. The use of time as a parameter in dealing with flow along a surface is obscure, but time can be easily eliminated by the use of c_r, the phase velocity of advance of a particular wave along the surface, that is, $dx = c_r \, dt$. By means of this relation it is possible to rewrite $\int \beta_i \, dt$ in terms of several dimensionless quantities that occur in the Pretsch charts:

$$\int_{t_n}^{t_1} \beta_i \, dt = \int_{(x/c)_n}^{(x/c)_1} \frac{\beta_i \delta^*}{U} \left[\left(\frac{U}{U_\infty} \right)^3 \frac{R_c}{R_{\delta^*}^2} \right] \frac{\alpha \delta^*}{\beta_r \nu} \, d\left(\frac{x}{c}\right) \qquad (4)$$

In certain respects group velocity is the proper velocity to consider for the reason that energy is propagated with group velocity. However, the phase velocity c_r, is so nearly independent of wave length that group velocity and phase velocity differ little. Hence for purposes of correlation there is little choice between the two, and the phase velocity is used because it is simpler.

The quantity $(U/U_{\infty})^3 R_c/R_{\delta^*}^2$ is a function only of the pressure distribution. Using Eq. (4), the procedure for calculating the amplification ratio of any particular dimensionless frequency is:

a) Select a value $(x/c)_1$ at a value of R_c for which the amplification factor is to be maximized.

b) Compute the necessary boundary-layer properties such as

$$R_{\delta^*}, \left[\left(\frac{U}{U_{\infty}}\right)^3 \frac{R_c}{R_{\delta^*}^2}\right], \text{ and } \beta \text{ versus } x/c.$$

c) Choose a value of $\beta_r \nu/U_{\infty}^2$. Try to choose one representing the frequency receiving the greatest amplification.

d) Compute $\beta_r \nu/U^2$ versus x/c from the relation

$$\frac{\beta_r \nu}{U^2} = \left[\frac{\beta_r \nu}{U_{\infty}^2}\right]\left[\frac{U_{\infty}^2}{U^2}\right]$$

e) For each x/c station, by means of the appropriate values of R_{δ^*} and $\beta_r \nu/U^2$, read $\beta_i \delta^*/U$ and $\alpha\, \delta^*$ from the proper β-chart. Interpolate between charts as necessary.

f) Enter the proper values into Eq. (4) for final evaluation. A five- to ten-step calculation of the integrand and subsequent integration by planimeter is of sufficient accuracy.

g) Repeat with other values of $\beta_r \nu/U_{\infty}^2$ until the highest value of the integral in Eq. (4) is found. If $(x/c)_1$ is the transition point, the value computed is $\int_{t_n}^{t_{tr}} \beta_i \, dt$, the natural logarithm of the amplification of the most critical frequency at transition.

It is hardly worth mentioning that the resulting answer is only a fictitious or apparent amplification factor, because near transition disturbances in the

boundary layer are large and no longer of the form of Tollmien-Schlichting waves. Since the theory is a small-perturbation theory, obviously it is not applicable close to transition. Nevertheless, calculations are made as if it were, on the premise that since they are valid early in the amplification process, they should account approximately for the factors influencing transition throughout the entire amplification process. Many other examples exist in which small-perturbation theory is used outside its domain of validity, the Prandtl-Glauert compressibility correction being one well known example.

Constant-β Flows

If a flow is of a constant-β type (this condition is necessary only in the unstable region), Pretsch's rate charts can be integrated once and for all to provide the full amplification ratio up to any value of R_{δ^*}. For two-dimensional flow his report (Ref. 19) contains such charts for $\beta = -0.198$, -0.10, 0, 0.2, 0.6, and 1.0. However, for our purposes they are not needed, for the reason that they provide a relation between β, R_{δ^*}, and $\int \beta_i \, dt$, and as a consequence the constant-β flow problem can be dealt with in terms of R_{δ^*}. The relations provided are presented in Fig. 3. In the basic Orr-Sommerfeld equation R_{δ^*} is a determinant of rate of growth of disturbances, not of strength. Only in cases of similar flows can such a parameter be used also as a measure of strength of disturbances.

A Sample Calculation

A sample calculation as applied to a body of revolution at $R_c = 6.65 \times 10^6$ is illustrated by Figs. 4, 5, and 6. The boundary-layer properties as computed by the method of Ref. 22 are shown in Fig. 4. Notice that the boundary layer becomes unstable for Tollmien-Schlichting waves near six percent of the chord whereas according to Fig. 6 the experimental transition point is near fifty percent of the chord at this Reynolds number.

The correlation problem requires computation of the apparent amplification ratio for the worst frequency at the measured transition point. Fig. 5a is a plot of the integrand of Eq. (4) for several values of $\beta_r \nu / U_\infty^2$ chosen

to be near the critical. The highest frequency responds first, but as the boundary layer thickens farther downstream a lower frequency receives the greatest amplification and the high-frequency receives the greatest amplification, or it may even decay. Furthermore, the amplification rate may grow and decay and then grow again according to the variation of β. Such an event is illustrated by the case $\beta_r \nu/U_\infty^2 = 2.5 \times 10^{-5}$. The decelerating flow beyond $X/c = 0.7$ so destabilizes the boundary layer that disturbances of this frequency receive new energy and commence rapid growth again.

Since the transition point is known to be at $X/c = 0.50$, we seek the maximum value of the integral up to this point. The insert in Fig. 5a is an auxiliary interpolation plot for determining the maximum value. It illustrates the considerable sensitivity of amplification to frequency.

In the converse problem of estimating the transition point, one must determine where the most critical frequency first reaches its limiting value, for example, e^9. Fig. 5b illustrates the procedure necessary now. One must construct the cumulative integral and study enough values of $\beta_r \nu/U_\infty^2$ to determine an approximate envelope. The results for a range of Reynolds numbers are shown in Fig. 6. Curves of $R_{\delta^*} = 3000$ and 5000, as well as curves for $\int \beta_i \, dt = 0$, 8, and 9, are shown in order to compare several different transition criteria. Notice that $\int \beta_i \, dt = 8$ predicts transition very accurately. Further discussion of this figure will be given in a later section.

RESULTS OF THE CORRELATION STUDY

Sources of Error

Before results are presented, it is advisable to point out the sources of error that enter into the present correlation effort. They are:

a) We fail to follow the principles of Eq. (1), that is, we evaluate only $a(R_{\delta^*})$.

b) Furthermore, $a(R_{\delta^*})$, or more precisely the apparent-fluctuation shear stress, is evaluated with different degrees of accuracy, depending on the pressure distribution. The sketch below illustrates one possible reason. The problem is to predict the location of

transition T for flows abc and abd. In either flow Tollmien-Schlichting waves begin amplifying at N. If their amplitude remains small up to P, the calculations are accurate to this point but will be of poor accuracy beyond. In flow abc we shall be applying erroneous calculations for a considerable distance. But in flow abd, because the final part of the flow is less stable, amplification rates will be greater. Even though the percentage accuracy in computation of growth rate is unchanged, a better estimate of T on abd will be provided, for the simple reason that the extent of inaccurate calculations is decreased.

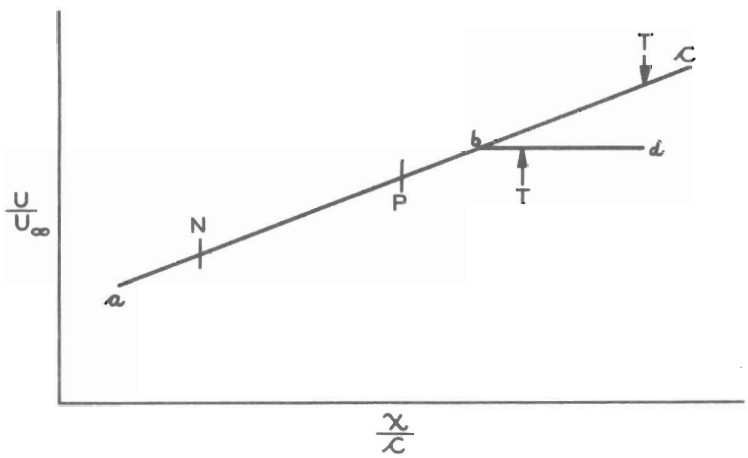

c) Since wave growth is computed by assuming that the boundary-layer profiles are Hartree profiles, their stability may be considerably in error.

d) The method of Ref. 22 predicts separation early. Therefore in decelerating flows one can expect $\int \beta_1 \, dt$ to be too high.

e) The Pretsch charts are inaccurate even for constant-β flows, and the accuracy deteriorates for negative β because the original solutions of the Orr-Sommerfeld equation are built upon the assumption that R_{δ^*} is large. For instance, according to Lin the neutral-stability limit for the Blasius boundary layer is $R_{\delta^* \text{ crit}} = 420$. Pretsch's value is 680. For Blasius flow a more nearly accurate amplification rate chart does exist, namely, Shens' (Ref. 38). By the time the boundary layer in Blasius flow has reached a thickness corresponding to $R_{\delta^*} = 3000$, the most critical

frequency will have been amplified by the factor $e^{6.4}$ according to Pretsch. But according to Shen the factor is e^{10}.

f) Because transition occurs over a region instead of at a point, its location was seldom accurately established; and since there is no standard definition of a transition point and its determination, there are inconsistencies among the results of various experimenters.

g) Wind tunnels always show a variation in turbulence with speed. Therefore tests in ordinary wind tunnels on the relation between Reynolds number and transition point are confused by this effect.

h) Additionally, it is probable that from tunnel to tunnel there are variations in the spectrum of turbulence, even though the R.M.S. value is nearly the same.

i) In many of the cases studied, the pressure distribution measurements were inadequate for the present type of work.

j) Surface finish and smoothness were not uniform from model to model.

k) Some models had definite flaws; some had too much waviness.

i) Finally, because Pretsch's charts are difficult to read, the random error of calculation is considerable.

Figure 7 and Table I

Adequate treatment of each case would demand a short essay on each data point, because of the great variety of conditions that influence the results. Obviously that is so much out of the question that we must be content with a chart, Fig. 7, and a table, Table I, listing certain key properties of the flow.

Since R_{δ^*} has long been used as a transition parameter, the results are plotted in two forms: $R_{\delta^*_{tr}}$ versus β and $\int \beta_i \, dt$ versus β. The points represent substantially a random sampling from nearly all of the applicable experiments. For example, some tests provide more than ten pairs of values of $\left[(x/c)_{tr}, R_c\right]$. Two or three values from such a test, roughly representing the extreme and mean conditions, were chosen. To the best of the writer's knowledge, the data represent virtually all test that are at sufficiently high Reynolds number and in very low-turbulence tunnels or flight. The types of cases covered are:

a) Bodies of revolution in low-turbulence wind tunnels
b) Airfoils in flight
c) A convex plate in a narrow low-turbulence channel
d) Airfoils in low-turbulence wind tunnels

The range of β shown on the plot for a particular case represents the variation between the point of neutral stability and the transition point. Ticks on the curves are used to provide a crude guide to the nature of the variation. Some flows are at constant β throughout the range, some begin the amplification at low β and end at a high β, others, vice versa, etc.

Table I and the data points can be related by coordinates of the points together with their symbols. Comments in the table provide further information about the data and their source. A measure of relative roughness is the Reynolds number per foot U_{∞}/ν, for if a roughness is constant (for example, No. 400 sandpaper finish) the ratio of roughness height to δ^* increases as U_{∞}/ν increases. For this reason both U_{∞}/ν and R_c are tabulated.

Sample Predictions

Since predicting transition is the practical goal of the study, we shall consider two typical examples, the NACA body of revolution of fineness ratio 9 (Ref. 23) and the NACA $65_{(215)}$-114 airfoil (Ref. 24). The first was chosen because it represents particularly good agreement between theory and experiment, and the second was chosen because it represents about average agreement.

The first example has already been presented for another purpose in Fig. 6. To estimate transition two methods are at once apparent:

a) Use of the amplification ratio, requiring the choice of $\int \beta_i \, dt$.
b) Conventional use of R_{δ^*}, requiring selection of a value from the upper part of Fig. 7.

In the several negative-β cases of Fig. 7 the values of $\int \beta_i \, dt$ are known to be too high because of the approximate method of boundary-layer calculation.

It will be seen later that a value of about e^9 is representative. The choice of R_{δ^*} for use in the second method is obscure, for if one wishes to estimate the position of transition as a function of R_c, it is apparent from Fig. 4 that both the mean and terminal β will vary with the location of the transition point. According to Fig. 4, if one tried to vary $R_{\delta^*_{tr}}$ with x/c_{tr} by following the trend of the lines $\int \beta_i \, dt = \text{const.}$, he would choose the highest value of R_{δ^*} for the highest value of R_c because the average or terminal value of β is highest. At the lowest Reynolds number he would choose the lowest value of R_{δ^*} as a criterion. But according to Table I and Fig. 7, that procedure would lead to results exactly opposite to experiment. This difficulty illustrates the objection to the estimation of transition by means of a relation between $R_{\delta^*_{tr}}$ and a gradient parameter, for there is no way of using it except a crude one. This crude way consists of selecting a value of β representative of the pressure distribution and then selecting a value of $R_{\delta^*_{tr}}$ corresponding to it from Fig. 3 or Fig. 7. In the experimental pressure distribution of Fig. 4, $\beta = 0$ would be a representative value and $R_{\delta^*_{tr}} = 3000$ corresponds to this value of β (Fig. 3 or Fig. 7). The consequences of these two choices for the two methods can be seen in Fig. 6. The method using $\int \beta_i \, dt = 8$ provides fine agreement; the result of using the other method and choice differs from the experimental result both in magnitude and shape. If one had not had the test values before him and had tried to vary R_{δ^*} with x/c according to the trend of the lines $\int \beta_i \, dt = \text{const.}$, the error would have been even greater, rather than less.

The second example fails to produce as satisfactory agreement. Curves corresponding to $\int \beta_i \, dt = 8$ and 10 have been included to provide a rough idea of the sensitivity of the result to the choice of $\int \beta_i \, dt$. Again values of $R_{\delta^*_{tr}}$ have been chosen, one being 3000, in order to emphasize the impossibility of using one universal value. The other is taken as 5000, because within the range of interest β varies between 0.092 and 0.148. On the upper surface β is constant forward of $x/c = 0.30$. On the lower, β equals 0.148 at the start of amplification and 0.092 at transition. Again, because the problem of how to read the chart of R_{δ^*} versus β arises, nothing better than a rough value of R_{δ^*} can be chosen.

The results are to be seen in Fig. 8. On the upper surface, the value $\int \beta_i \, dt = 9$ predicts the transition point within 5-percent chord. Here, forward of 0.30c, both the R_{δ^*} and $\int \beta_i \, dt$ methods produce the same shape of curve, because β is constant. On the lower surface the error is greater, being about 7-percent chord. Hence neither method has the desired accuracy, but again the value $R_{\delta^*} = 3000$ used on the body of revolution is quite unacceptable. The accuracy of the experimental results is not high, for if one examines Fig. 4 of Ref. 24 he sees that R_c corresponding to a particular location of transition could be determined only to within 2 or 3 million.

DISCUSSION

Miscellaneous Observations

From a study of Figs. 6, 7, and 8 and Table I the following facts are observable. There is a strong variation of $R_{\delta^*_{tr}}$ with β; in fact, it varies quite as predicted by stability theory. Upon making allowance for erroneously high values of $\int \beta_i \, dt$ in the negative-β region, $\int \beta_i \, dt$ appears to be independent of β. Unfortunately, the large scatter in the data is enough to reduce confidence in these observations but not enough to invalidate them. Therefore it can be said that the Tollmien-Schlichting excitation process dominates the flow sufficiently to determine the transition point when roughness, turbulence, and other extraneous influences are absent. This fact appears true even though the waves may not be two-dimensional, as is assumed in the usual form of the theory.

The large scatter observable in Fig. 7 is an indication of inadequate calculation methods, insufficiently controlled and instrumented experiments, and great sensitivity of transition to numerous extraneous factors such as roughness and waviness.

There is substantial agreement between the results of tests in flight and tests in a good low-turbulence wind tunnel.

There is no evidence that zero roughness and zero turbulence will delay

transition appreciably, or in other words that $\int \beta_i \, dt$ at transition can be increased markedly by additonal care. All the models listed are of high quality. Moreover, some of the tests are in free flight where the turbulence is substantially zero. This statement that still smoother models and reduced turbulence will not delay transition much more is only an empirical observation of course, for Eq. (1) indicates no limit to $\int \beta_i \, dt$. Instead, it indicates that the product of neutral-disturbance amplitude and amplification ratio must be constant. If the disturbance amplitude at the neutral point were continually reduced, one could expect a compensating increase in $\int \beta_i \, dt$. But such further reduction appears impossible in practice, because of the exponential nature of $a(R_{\delta^*})$. An increase of only 3 in the value of $\int \beta_i \, dt$ represents a decrease by a factor of $1/e^3$, that is, 1/20, in the amplitude at the neutral point.

Stability theory adequately correlates transition in two-dimensional and axially symmetric flow. On the basis of $R_{\delta^*_{tr}}$ as a criterion, one could expect considerable laminar flow on a body of revolution, because the expansion of the body thins the boundary layer, at least back to the maximum diameter. However, the thinning process also destabilizes the boundary layer. These two effects oppose each other, and only the stability theory properly accounts for both effects at once.

Although the number of cases represented in Fig. 7 is too large for detailed treatment, some discussion of a few examples will be given in order to bring out the meaning of the various data points.

First consider Leipmann's tests (Ref. 25) -points 1-7, Table I. Liepmann used a flat plate in a narrow channel of 8:1 aspect ratio to measure the transition point in Blasius flow. The channel was so small that the free-stream turbulence gradually increased along its length, which may explain why $\int \beta_i \, dt$ at transition is 5.4 instead of 6.5, as in Schubauer and Skramstad's test. In his experiments on the effect of pressure gradient, Liepmann again used the same type of channel.

Two points, 29, 30, are shown for the NACA 35-215 airfoil (Ref. 26). The

upper surface was resanded several times to bring it to the highest possible quality and minimum waviness. In the process, transition was moved back from X/c = 0.325 to 0.424. This example strikingly illustrates the sensitivity to surface quality and the problem of scatter seen in Fig. 7. Point 30 represents the bottom side of this wing, which did not receive the careful treatment given the top side-hence its lower value of $\int \beta_i \, dt$.

Point 24, for the British Hawker Hurricane fighter (Ref. 27 and 28) is interesting. Over most of the chord the flow was accelerating, but just before transition, it began a rapid deceleration (see Fig. 9). Here is a case in which R_{δ^*} grows to large values in a favorable β-environment, but in which transition occurs shortly thereafter in a strongly decelerating region. Naturally R_{δ^*} can reach a very large value at negative β's under such circumstances.

In the plot of $\int \beta_i \, dt$ versus β the situation, though not so bad, is still not good. The large value, 14.3, is due partly to the methods of calculation, as was already mentioned. It is of interest to note, however, that the transition point for this particular case would be predicted rather accurately, were one to use $\int \beta_i \, dt$ equal to 9 because the rate of growth of $\int \beta_i \, dt$ with x/c in the decelerating region is so great that the difference between the results for the values 9 and 14.3 represents only a small increment in x/c. In fact, 2-percent chord forward of the experimental transition point the amplification ratio has fallen to 10 (see Fig. 9).

Waviness

In each correlation study the effect of waviness was a question. Experimentally it has a large effect, as was mentioned in discussing the NACA 35-215 airfoil tests. An interesting problem would be the application of the present methods to the flow along sinusoidally-waved walls of various amplitudes in order to learn the effect on the calculated transition point. Such a study could be made by the methods of this article, but the significance of the results would be questionable. Görtler (Ref. 29) has supplied perhaps the most accurate calculation of the steady boundary-layer flow along such a wall. The steady-state calculations in themselves show a strong sensitivity

to the wall waviness. The next step, calculation of the amplification ratio, is questionable, because the boundary-layer profiles so little resemble the Hartree profiles. Therefore at this time one must be content with the following crude example to indicate the effect of waviness. Consider a flow having β = constant = 0.05. Then, assuming transition occurs at $\int \beta_i \, dt = 9$, we see from Fig. 3 that $R_{\delta^*} = 4550$. Now assume that the surface has waves such that $\beta = -0.05$ half the distance and $\beta = +0.15$ the other half, so that the mean value of β remains at $+0.05$. It is easy to show that a sinusoidal wall will exhibit such regions of decelerating flow even with very shallow waves. Now reading the line $\int \beta_i \, dt = 9$ on Fig. 3 at $\beta = -0.05$ and at $+0.15$, we find $R_{\delta^*} = 2250$ and 6250, respectively, giving an average value of 4250. Because the waviness is small, the boundary layer will grow at about the same average rate as in the smooth case. Therefore when the above values of R_{δ^*} are inserted in the R_{δ^*}, x relation, we find x_{tr} reduced approximately as follows:

$$\frac{x_{tr\ wavy}}{x_{tr\ smooth}} = \frac{R^2_{\delta^*\ wavy}}{R^2_{\delta^*\ smooth}} = \left(\frac{4250}{4550}\right)^2 = .87$$

In one particular case studied, a wave whose length L was 0.04c and whose crest was located at 0.22c, required only an amplitude of 0.001 L in order to approximate the aforementioned numerical values! The above example is of no great quantitative significance, but it is sufficiently definite to demonstrate that a strong effect of waviness is indicated by the theory.

Conflicts in Theories

Several interesting contradictions are created by the two opposing theories. According to the R_{δ^*} criterion, thinning a boundary layer should always delay transition, provided the thinning process can be done without unduly disturbing the boundary layer. Contrariwise, thickening should only hasten transition. According to stability theory the answer is not so clear. In a favorable gradient, thinning destabilizes the boundary layer and thickening stabilizes it. The problem is: which is reduced faster, $R_{\delta^*\ actual}$ or $R_{\delta^*_{tr}}$? If $R_{\delta^*_{tr}}$ is reduced faster than $R_{\delta^*\ actual}$, then thinning would

theoretically advance transition. Perhaps the simplest way of explaining the effect is by reference to Pohlhausen's parameter λ_P. Schlichting and others have computed the curve of $R_{\delta^*_{cr}}$ versus λ_P for the Pohlhausen profiles (Ref. 30), just as Pretsch has done for the Hartree profiles. Now $\lambda_P = (\delta^2/\nu)\, dU/dx$; if $dU/dx > 0$, reducing δ by a fraction n will reduce λ_P by an amount n^2, since dU/dx and ν are unaffected by the operation. The same effect applies in the β-system, but the relations are more obscure. The effect was studied briefly by the writer about 1949, and later a detailed study was made by Tetervin (Ref. 31). These considerations explain why on bodies of revolution transition is at a lower value of R_{δ^*} than it is on two-dimensional shapes.

Another problem is mentioned to illustrate the difference in answers supplied by the two methods. Assume that transition occurs when R_{δ^*} exceeds a specified value, say $(R_{\delta^*})_1$. Now assume that a boundary layer of the proper type gradually grows in the flow along the plate. At some point x_1, $(R_{\delta^*})_1$ will be exceeded, and at that point transition should begin. Now shortly before x_1 let us modify the flow by a combination of pressure gradient and area suction so that R_{δ^*} is held just below the value $(R_{\delta^*})_1$, that is, at a value $(R_{\delta^*})_1 - \epsilon_1$, where ϵ_1 is a small number. The R_{δ^*} criterion will predict that transition never occurs. The $\int \beta_i\, dt$ criterion predicts that transition will be delayed only an infinitesimal amount, since if R_{δ^*} is maintained at the value $(R_{\delta^*})_1 - \epsilon_1$, the rate of growth of disturbances is reduced only by an infinitesimal amount, with the result that $\int \beta_i\, dt$ reaches its prescribed limit at the location $x_1 + \epsilon_2$, where ϵ_2 is another small number. Here we have a physically conceivable method of delaying the transition point. In the limit one method predicts an infinite delay in the transition point; the other predicts zero delay!

EVALUATION OF $\int \beta_i\, dt = 9$ AS A TRANSITION PARAMETER

In Fig. 7 no discernible trend of $(\int \beta_i\, dt)_{tr}$ with β is seen, but there is a large scatter. If a correlation parameter is sensitive, correlation studies may look poor and yet the parameter may be excellent for the practical

problem of prediction. Because sensitivity was apparent during the analysis of the test data, it was decided to test the parameter by selecting one representative value of $\int \beta_i \, dt$ and then to use it to predict the location of transition for all the cases of Table I.

Fig. 10 compares with measurement the predictions so made. The correlation is unusually good, in view of the nature of the data, the methods of calculation, and the large variation in $R_{x_{tr}}$. The points are identified by the same symbols used in Table 1, as well as by the measured values of $R_{x_{tr}}$. The lowest point represents the sphere. For it, most of the amplification of disturbances occurs in a region of strong adverse gradient, and here the amplification-rate charts are especially poor. Nevertheless a calculation was attempted, and much to everyone's surprise the measured and calculated values agreed remarkably well. Standard deviations have been computed separately for the two-dimensional and the body of revolution data. The values are tabulated on the figure. Because there are few signs of bias, the value $\int \beta_i \, dt = 9$ appears to be the best integral value. It is noteworthy that a similar constant amplification ratio was found for the growth of Taylor-Görtler vortices along a concave surface (Ref. 32). In that case the amplification factor was almost the same, namely, e^{10}.

A SHORT-CUT METHOD (MICHEL'S METHOD)

For any velocity distribution there is a unique relation between $R_\theta = U\theta/\nu$ and $R_x = Ux/\nu$. If the flows are similar flows, the relation is $R_\theta = p\sqrt{R_x}$ (Ref. 21) where p is a constant for a particular value of β. The relation is plotted in Fig. 11. for several values of β. For higher values of β, which correspond to the more stable flows, R_θ is lower at any particular value of R_x. The reason is easily seen from the sketch below, comparing two flows having different degrees of stability, flow A being the one with low stability.

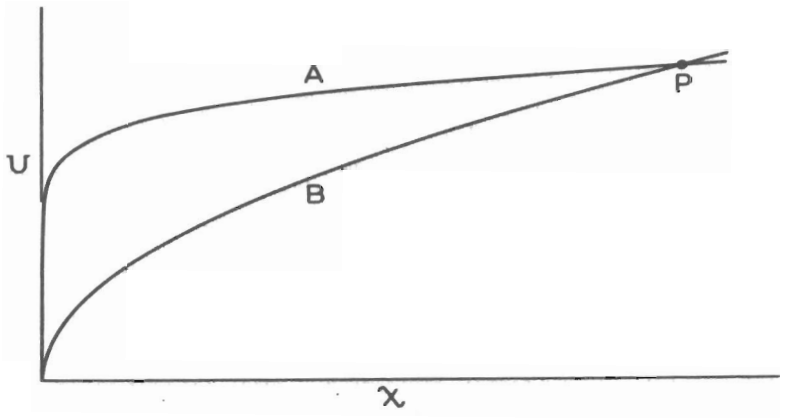

At the point P both flows will have the same value of R_x, because U and x are equal. But in flow B the velocity in the forward portions is lower than in flow A, and therefore the skin friction of flow B and consequently θ and R_θ are less. Hence it is qualitatively apparent that a low value of R_θ at a given value of R_x is a sign of greater stability of the boundary layer, even when the flows are not similar flows.

On each of the lines for the similar flows a particular point corresponds to $\int \beta_i \, dt = 9$ (Fig. 11). Now consider more general velocity distributions. Each will define a curve in the (R_θ, R_x)-plane, but in general the curve will not now be a straight line. On this curve a certain point will correspond to $\int \beta_i \, dt = 9$ and if the velocity distributions do not differ greatly from similar flows, it can be expected that the locus of $\int \beta_i \, dt = 9$ will be in good agreement with that of the similar flows. Hence a relation between $R_{\theta tr}$ and $R_{x tr}$ can serve as a rough measure of the stability of the boundary layer. It is not to be construed, however, that Michel's method of correlation will always supply approximately the deductions or predictions of stability theory. For example, consider again the problem of flow along a plate having a combination of area suction and adverse pressure gradient (p. 25). For this situation Michel's method will predict an infinite delay of the transition point.

Experimental data must be studied to obtain an indication of spread of data caused by non-similar velocity distributions. Such a study has been made of all the flows of Table I, and points corresponding to calculated values of $\int \beta_i \, dt = 9$ are plotted in Fig. 11. In most cases they deviate little from

the points provided by the similar flows. The points for bodies of revolution are plotted in terms of the equivalent two-dimensional flow as determined by Mangler's transformation. The reason most points agree reasonably well with those provided by the similar flows is that for most flows of technical importance the velocity distribution retains a resemblance to one of the similar flows. But at times there may be a considerable difference, as is illustrated by the sphere. $R_{x_{tr}}$ for the sphere is so low that in the similar flow having the same value of $R_{x_{tr}}$, β is about - 0.10. This β-flow has a constantly decreasing velocity, starting with $U = \infty$ at $x = 0$. But the sphere begins with a stagnation flow so that $U = 0$ at $x = 0$, and here the two flows bear no resemblance to each other.

Therefore it becomes possible to prepare a correlation curve in the (R_θ, R_x)-plane that will provide rather good results as long as the velocity distributions are rather smooth curves, having little undulation, and provided they resemble those that provided the data for the original correlation. The above discussion explains why Michel's correlation was successful. Michel's curve, points for similar flows, and points for the flows of Table I are all shown in Fig. 11.

For purposes of defining a curve to be used in locating the transition point, it is slightly better to work directly from the test data and thus avoid errors introduced by errors in the calculation of the amplification ratio. Fig. 12 is such a plot. The difference between Figs. 11 and 12 is that Fig. 11 is based on data calculated by the basic method and Fig. 12 uses the measured data.

Within the range of the data a straight-line fit is as good as any other. The line shown is defined by the equation:

$$R_{\theta_{tr}} = 1.174\, R_x^{0.46} \qquad 0.3 \times 10^6 < R_x < 20 \times 10^6 \qquad (5)$$

Shown also is Michel's original curve. Both Michel's and the proposed locus are of an insensitive nature for the reason that their slopes are nearly the

the same as those of the boundary layer itself in this plane. Hence the data show little scatter and look good on the plot, but the accuracy may not be as great as might be expected, for the reason that $R_{x_{tr}}$ must be determined by finding the intersection with the transition locus of the (R_θ, R_x)-curve of the boundary layer under consideration. Because the curves frequently intersect at quite a shallow angle, $R_{x_{tr}}$ may be considerably in error. Comparison of the transition locus with the data of Fig. 11 shows that $\int \beta_i \, dt = 9$ indeed predicts the locus with a high degree of accuracy.

The best means of evaluating this short method is to compare with measurement the transition points calculated by means of Eq. (5). That has been done for all points used in Fig. 10.and results are given in Fig. 13. In two-dimensional flow the method is substantially equal in accuracy to that of the basic method and of course is much faster, for the reason that it requires only the calculation of R_θ and R_x along the body, completely bypassing the stability calculations. Standard deviations are shown for comparison with those on Fig. 10. Mangler's transformation apparently correlates results for bodies of revolution, but the accuracy is poor.

CONCLUSIONS

1. Stability theory successfully explains the effect of pressure gradient on the transition point in low-speed flows of very low-turbulence streams past very smooth bodies, either axially symmetric or two-dimensional.
2. By the time the transition point is reached, the most critical Tollmien-Schlichting wave has undergone an apparent amplification of about e^9 times, its amplitude at the beginning of its growth. Of course, this value is based on Pretsch's set of stability charts; improved charts may change the value of the factor.
3. By means of this constant, e^9, it is possible to predict the transition point in arbitrary flows with an error in $R_{x_{tr}}$ seldom greater than 20 percent.
4. Evidently, in view of the above successful correlation, the unstable,

self-energizing mechanism of Tollmien-Schlichting waves is the dominating process during the initial stages of the evolution of a boundary layer from a laminar to a turbulent state, provided the flow meets the limitations of this report.

5. The considerable body of data examined indicates that the extent of laminar flow obtainable in good low-turbulence tunnels is no less than that obtainable in flight.
6. The experimental data demonstrate that R_{δ^*} and R_{θ} do not have constant values at the transition point. Rather, $R_{\theta_{tr}}$ and $R_{\delta^*_{tr}}$ are variable but can be correlated approximately by Michel's method in most cases of interest.
7. Stability theory supplies the explanation for Michel's hitherto unexplained transition-correlation curve.
8. Michel's correlation method is extended by means of Mangler's transformation to include axially symmetric flows but the results have a low degree of accuracy.
9. The data and studies of this report justify Michel's method as a rapid, approximate method for estimating the transition point in two-dimensional flow so long as the velocity distribution of the problem roughly resembles one of the distributions used in the original correlation.

REFERENCES

1. Jones, B. Melvill: Flight Experiments on the Boundary Layer. Jour. Aero. Sci., vol.5, no. 3, Jan. 1938, pp. 81-100.

2. Taylor, G. I.: Statistical Theory of Turbulence, V-Effect of Turbulence on Boundary Layer, Theoretical Discussion of Relationship Between Scale of Turbulence and Critical Resistance of Spheres. Proc. Roy. Soc. A., vol. 156, no. 888, Aug. 17 1936, pp. 307-317.

3. Hall, A. A. and Hislop, G. S.: Experiments on the Transition of the Laminar Boundary Layer on a Flat Plate. British R and M no. 1843, 1938.

4. Fage, A. and Preston, J. H.: On Transition from Laminar to Turbulent Flow in the Boundary Layer. Proc. Roy. Soc. A., vol. 178, no. 973, June 12 1941, pp. 201-227.

5. Schlichting, H.: Boundary Layer Theory. McGraw Hill, New York, First English Ed., Chaps. XVI, XVII, 1955.

6. Gruschwitz, E.: Die turbulente Reibungsschicht in ebener Strömung bei Druckabfall und Druckanstieg. Ingenieur-Archiv., vol. II, Sept. 1931, pp. 321-346.

7. Schubauer, G. B. and Skramstad, H. K.: Laminar-Boundary-Layer Oscillations and Transition on a Flat Plate. NACA TR 909, 1948.

8. Emmons, H. W.: The Laminar-Turbulent Transition in a Boundary Layer, Part I. Jour. Aero. Sci., vol. 18, July 1951, pp. 490-498.

9. Emmons, H. W. and Bryson, A. E.: The Laminar-Turbulent Transition in a Boundary Layer. Proc. 1st U.S. Nat. Cong. Theor. and App. Mech., 1950 pp. 859-868.

10. Schubauer, G. B. and Klebanoff, P. S.: Contributions on the Mechanics of Boundary-Layer Transition. NACA TN 3489, Sept. 1955.

11. Bennett, H. W.: An Experimental Study of Boundary Layer Transition. Rept. prepared for Off. Naval Res., Contract Nonr-673(00) by Kimberly-Clark Corp., Sept. 1953. Also available as ASTIA Doc. AD no. 18,379.

12. Wortmann, F. X.: Eine Methode zur Beobachtung und Messung von Wasserströmungen mit Tellur. Z. f. angew. Physik., bd. 5, heft 6, June 1953, pp. 201-206.

13. Görtler, H. and Tollmien, W.: 50 Jahre Grenzschichtforschung. Friedr. Vieweg, Braunschweig, 1955.

14. Laufer, John: Experimental Observation of Laminar Boundary-Layer Oscillations in Supersonic Flow. Jour. Aero. Sci., vol. 23, no. 2, Feb. 1956, pp. 184-185.

15. Michel, R.: Etude de la Transition sur les Profils D'Aile-Establissement d'un Critere de Determination du Point de Transition et Calcul de la Traînee de Profil en Incompressible. ONERA Rapport 1/1578A, July 1951.

16. Dryden, H. L.: Transition from Laminar to Turbulent Flow at Subsonic

and Supersonic Speeds. Pres. at Conf. on High-Speed Aero, Poly. Inst. of Brooklyn, Jan. 20 1955.

17. Liepmann, H. W.: Investigation of Boundary Layer Transition on Concave Walls. NACA Wartime Rept., ACR no. 4J28, Feb. 1945.

18. Pretsch, J.: The Excitation of Unstable Perburbations in a Laminar Friction Layer. NACA TM 1343, Sept. 1952.

19. Pretsch, J.: Calculation of the Limit of Stability of Boundary Layer Profiles and of the Amplification of Disturbances. A.V.A. Monographs, British R and T no. 1004, March 15 1948.

20. Pretsch, J.: The Stability of Two-Dimensional Laminar Flow with Pressure Drop and Pressure Rise. Jahrbuch d. Deutschen Luftfahrtforschung, I, 1941, pp. 158-175. Also available as British R and T no. 22, File No. B.I.G.S.-37, Jan. 1946.

21. Smith, A. M. O.: Improved Solutions of the Falkner and Skan Boundary-Layer Equation. Sherman Fairchild Fund Paper No. FF-10. Inst. Aero. Sci., March 1954.

22. Smith, A. M. O.: Rapid-Laminar Boundary Layer Calculations by Piecewise Application of Similar Solutions. Accepted for pub. in Jour. Aero. Sci.

23. Boltz, F. W., Kenyon, G. C. and Allen, C. Q.: Measurements of Boundary-Layer Transition at Low Speed on Two Bodies of Revolution in a Low Turbulence Tunnel. NACA RM A56G17, 1956.

24. Braslow, A. L. and Visconte, F.: Investigation of Boundary-Layer Reynolds Number for Transition on an NACA $65_{(215)}$-114 Airfoil in the Langley Two-Dimensional Low-Turbulence Pressure Tunnel. NACA TN 1704, Oct. 1948.

25. Liepmann, H. W.: Investigations on Laminar Boundary-Layer Stability and Transition on Curved Boundaries, NACA Wartime Rept., ACR 3H30, Aug. 1943.

26. Wetmore, J. W., Zalovcik, J. A. and Platt, R. C.: A Flight Investigation of the Boundary-Layer Characteristics and Profile Drag of the NACA 35-215 Laminar-Flow Airfoil at High Reynolds Numbers. NACA Wartime Rept.

no. L-532, May 1941.

27. Plascott, R. H., Higton, D. J., Smith, F. and Bramwell, A. R.: Flight Tests on Hurricane II, Z. 3687 Fitted with Special Wings of 'Low-drag' Design. British R and M no. 2546, 1952.

28. Davies, H.: Some Aspects of Flight Research. Jour. Roy. Aero. Soc., vol. 55, no. 486, June 1951, pp. 325-361.

29. Görtler, H.: Einfluss einer schwachen Wandwelligkeit auf den Verlauf der laminaren Grenzschichten. Teil I, Z. angew. Math. Mech., bd. 25/27, nr. 8/9, Nov./Dec. 1947; Teil II, Z. Angew. Math. Mech., bd. 28, nr. 1, Jan. 1948.

30. Schlichting, H.: Lecture Series 'Boundary Layer Theory' Part II-Turbulent Flows. NACA TM no. 1218, April, 1949.

31. Tetervin, N.: A Study of the Stability of the Incompressible Laminar Boundary Layer on Infinite Wedges, NACA TN no. 2976, Aug. 1953.

32. Smith, A. M. O.: On the Growth of Taylor-Görtler Vortices Along Highly Concave Walls. Quart. App. Math., vol. XIII, no. 3, Oct. 1955, pp. 233-262.

33. von Doenhoff, A. E.: Investigation of the Boundary Layer About a Symmetrical Airfoil in a Wind Tunnel of Low Turbulence. NACA Wartime Rept. no. L-507, August 1940.

34. Fage, A.: Experiments on a Sphere at Critical Reynolds Numbers. British R and M no. 1766, Sept. 1936.

35. Zalovcik, J. A. and Skoog, R. B.: Flight Investigation of Boundary-Layer Transition and Profile Drag of an Experimental Low-Drag Wing Installed on a Fighter-Type Airplane. NACA Wartime Rept. ACR L5C08a, April 1945.

36. Smith, M. A. and Higton, D. J.: Flight Tests on 'King Cobra' FZ. 440 to Investigate the Practical Requirements for the Achievement of Low-Drag Coefficients on a 'Low-Drag' Aerofoil. British R and M no. 2375, 1950.

37. Jacobs, E. N.: Preliminary Report on Laminar-Flow Airfoils and New Methods Adopted for Airfoil and Boundary-Layer Investigations, NACA Wartime Rept. no. L-324, June 1939.

38. Shen, S. F.: Calculated Amplified Oscillations in the Plane Poiseuille and Blasius Flows. Jour. Aero. Sci., vol. 21, no. 1, Jan. 1954, pp. 62-64.

TABLE I SUMMARY DATA ON CASES STUDIED

SYMBOL	CASE NO.	$\beta_{MIN.}$	$\beta_{MAX.}$	$\beta_{NEUT.}$	β_{tr}	$R_{x_{tr}}$ $\times 10^{-6}$	$R_{\theta_{tr}}$ †	$R^{*}_{\beta_{tr}}$	$\int \beta_i \, dt$	NEUT. POINT x/c	TRANSITION POINT x/c	R_c $\times 10^{-6}$	U_∞/ν $\times 10^{-6}$ ft^{-1}	BODY	TEST FACILITY	REFERENCE	COMMENTS
⊡	1	-.065	.035	.000	-.065	1.49	824	2230	5.3	.067	.666	2.28	.386	CURVED PLATE PRESS. DIST. B	SPECIAL LOW TURBULENCE CHANNEL	25	NARROW CHANNEL CAUSED TURBULENCE TO INCREASE WITH DISTANCE DOWNSTREAM
⊡	2	-.065	.135	.000	.040	1.53	803	2040	5.6	.100	.970	1.60	.272				
⊡	3	-.120	.000	.000	-.120	1.18	753	2160	18.6	.058	.333	3.69	.626	CURVED PLATE PRESS. DIST. C			
⊡	4	-.172	-.020	-.020	-.100	.520	521	1460	—	.128	.889	0.66	.113				
⊡	5	.000	.500	.010	.500	2.97	1080	2480	4.2	.085	.950	3.27	.554	CURVED PLATE PRESS. DIST. D			
⊡	6	.000	.325	.005	.020	2.69	1040	2660	4.2	.038	.639	4.57	.774				
⊡	7	.000	.000	.000	.000	2.50	1050	2720	5.4	—	Variable	Variable	Variable	FLAT PLATE CONST. VELOCITY			
△	8	.000	.000	.000	.000	2.84	1120	2900	6.5	—	Variable	Variable	Variable		N.B.S. WIND TUNNEL	7	EXCELLENT DATA
◺	9	.013	.100	.100	.013	13.6	2230	5740	10.1	.058	.414	25.0	3.53	NACA $65_{(215)}$-114 AIRFOIL, TOP	NACA TDPT	24	EXCELLENT DATA WAVINESS AT x/c = .37
◺	10	.055	.100	.100	.055	15.8	2360	5950	10.8	.046	.346	35.0	4.94				
◺	11	.100	.100	.100	.100	16.0	2400	5960	10.0	.037	.291	45.0	6.36				
◺	12	.092	.148	.148	.092	14.3	2250	5600	10.2	.102	.470	25.0	3.53	NACA $65_{(215)}$-114 AIRFOIL, BOTTOM			
◺	13	.092	.148	.148	.092	16.3	2370	5900	11.0	.075	.385	35.0	4.94				
◺	14	.092	.148	.148	.092	16.2	2370	5900	8.9	.060	.300	45.0	6.36				
◈	15	-.160	.030	.030	-.160	1.40	865	2490	—	.144	.490	2.5	.50	NACA 0012 AIRFOIL, $\alpha = 0°$	NACA LOW TURB. TUNNEL	33	CALCULATED PROFILES (HARTREE) ARE LESS STABLE THAN EXPERIMENTAL
◈	16	-.110	.050	.050	-.110	2.08	953	2700	13.5	.116	.355	5.0	1.00				
◈	17	-.100	.060	.060	-.100	2.64	1050	2950	14.2	.103	.320	7.0	1.40				
◎	18	.005	.020	.020	.005	3.34	823	2300	7.6	.050	.300	10.9	1.36	BODY OF REV. F.R. =9:1 ELLIPSOID	NACA 12 FT. L.T. PRESS. TUNNEL	23	EXCELLENT DATA STING MOUNTED MODEL
◎	19	-.002	.020	.010	-.002	3.38	987	2530	7.5	.060	.500	6.6	.83				
◎	20	-.027	.020	.020	-.027	3.71	1100	3200	7.8	.103	.700	5.2	.65				
◎	21	-.040	.033	.033	-.040	4.45	967	2800	8.5	.092	.305	14.0	.93	N.P.L. BODY OF REV. F.R. =10	N.P.L. 13' x 9' WIND TUNNEL	PERSONAL COMMUNICATION	TUNNEL TURBULENCE SOMEWHAT HIGH
◎	22	-.085	.033	.033	.010	2.92	944	2430	10.0	.132	.457	6.3	.42				
◈	23	-.198	0	0	-.050	.57	355	1300	—	.780	.960	.424	—	6" DIA. SPHERE	N.P.L.	34	TUNNEL TURBULENCE NOT LOW
●	24	-.160	.175	.175	-.160	11.4	2140	6630	14.3	.216	.522	16.4	2.39	HURRICANE LOW DRAG WING	R.A.E. FLIGHT TEST	27, 28	C_L =.14
●	25	.030	.222	.173	.110	12.7	2070	5100	7.3	.200	.480	19.6	2.86				C_L =.10
◗	26	.061	.061	.061	.061	9.40	1910	4810	9.4	.028	.508	14.8	2.01	XP-47F R.H. WING LOW DRAG AIRFOIL	NACA FLIGHT TEST	35	C_L =.20, M =0.46 EXCELLENT DATA
◗	27	-.199	.129	.129	-.199	13.7	2400	9660	14.1	.103	.669	17.0	2.42	KING COBRA - NACA 66 SERIES WING, TOP	R.A.E. FLIGHT TEST	28,36	C_L =.15, ESTIMATED PRESS. DIST.
◗	28	-.199	.153	.121	-.199	13.0	2130	8590	20.9	.096	.668	17.0	2.42	KING COBRA - NACA 66 SERIES WING, BOTTOM			
▼	29	.064	.332	.142	.332	15.4	2300	5400	11.2	.090	.453	26.7	1.57	NACA 35-215 AIR-FOIL GLOVE, TOP	NACA FLIGHT TEST	26	$C_L \pm .238$, UPPER SURFACE WAS EXCELLENT
▼	30	.083	.083	.083	.083	10.2	1940	4850	8.4	.026	.299	26.8	1.58	NACA 35-215 AIR-FOIL GLOVE, BOTTOM			$C_L \pm .238$, LOWER SURFACE INFERIOR TO UPPER
⌂	31	—	—	—	—	—	—	—	—	—	—	—	—	ORIGINAL NACA LOW DRAG AIRFOILS	NACA LOW TURB. TUNNEL	37	NUMEROUS AIRFOILS, PRESS. DIST. DATA INCOMPLETE
+	32	-.050	.050	.050	-.050	2.73	1070	2860	8.7	.067	.296	9.45	1.05	9 FT. FLAT PLATE, 2½ IN. THICK $\alpha = ½°$	DOUGLAS EL SEGUNDO LOW TURB. W. T.	——	W.T. TEST SECTION ONLY 4FT. LONG.
⊗	33	.024	.072	.025	.034	3.72	652	2200	6.0	.053	.226	16	2.00	BODY OF REV. F. R. =7.5 : 1	NACA 12 FT. L. T. PRESS. TUNNEL	23	EXCELLENT DATA STING MOUNTED MODEL
⊗	34	-.005	.072	.025	-.005	4.14	1000	2660	5.8	.085	.499	8	1.00				
⊗	35	-.198	.072	.025	-.198	4.33	1170	6470	10.5	.127	.851	5	.62				

† —IN TRANSFORMED COORDINATE SYSTEM FOR BODIES OF REVOLUTION

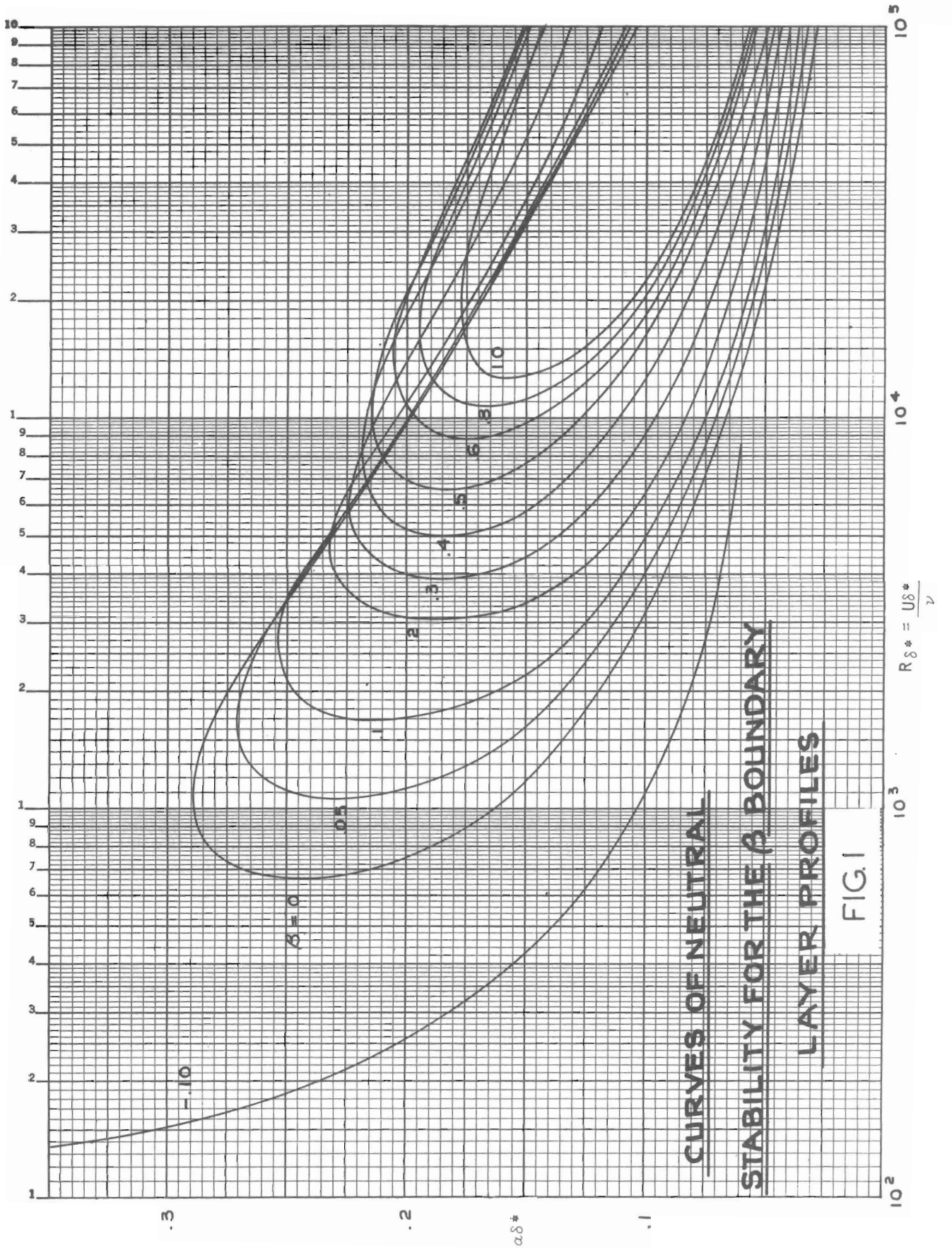
CURVES OF NEUTRAL STABILITY FOR THE β BOUNDARY LAYER PROFILES
FIG. 1
β = 0
0.5
1
2
3
4
5
6
8
10
-.10
$R_{\delta^*} = \frac{U\delta^*}{\nu}$
$\alpha\delta^*$

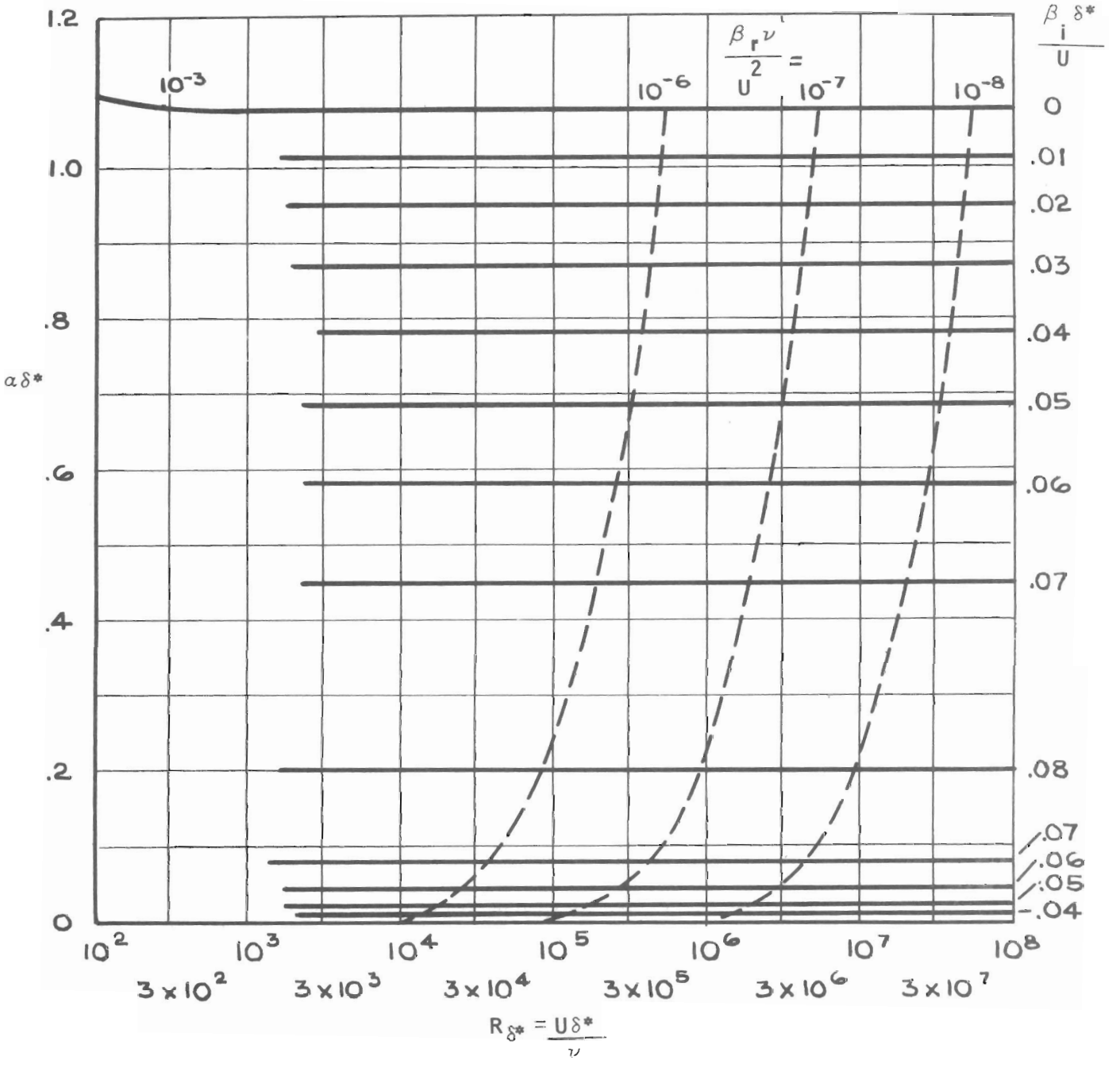

CURVES OF AMPLIFICATION RATE
FOR THE β BOUNDARY LAYER PROFILES
$\beta = -.198$
FIG. 2a

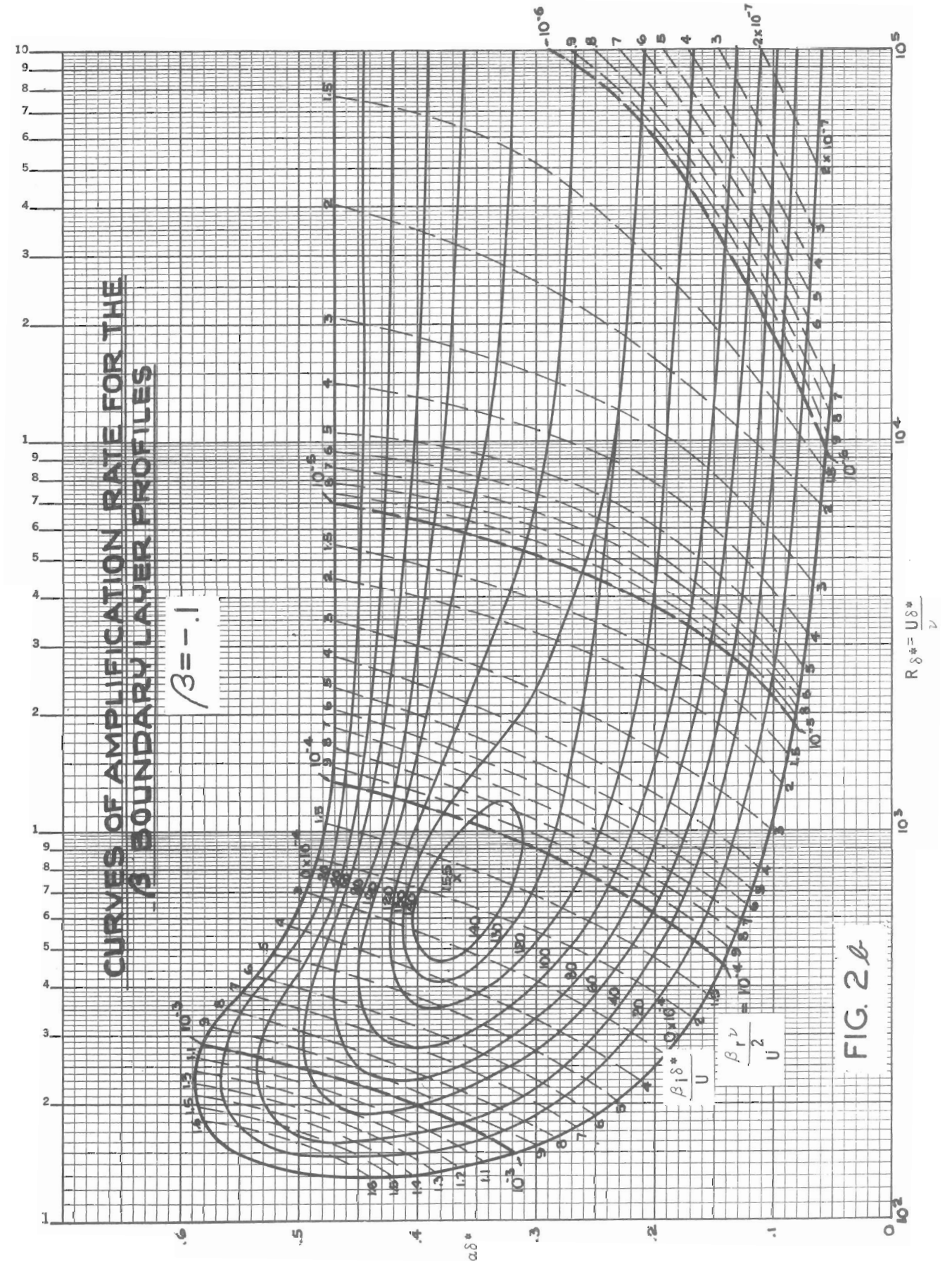
CURVES OF AMPLIFICATION RATE FOR THE
2 BOUNDARY LAYER PROFILES
β = -.1
$\alpha\delta^*$
$R_{\delta^*} = \frac{U\delta^*}{\nu}$
$\frac{\beta_i \delta^*}{U}$
$\frac{\beta_r \nu}{U^2}$

FIG. 2b

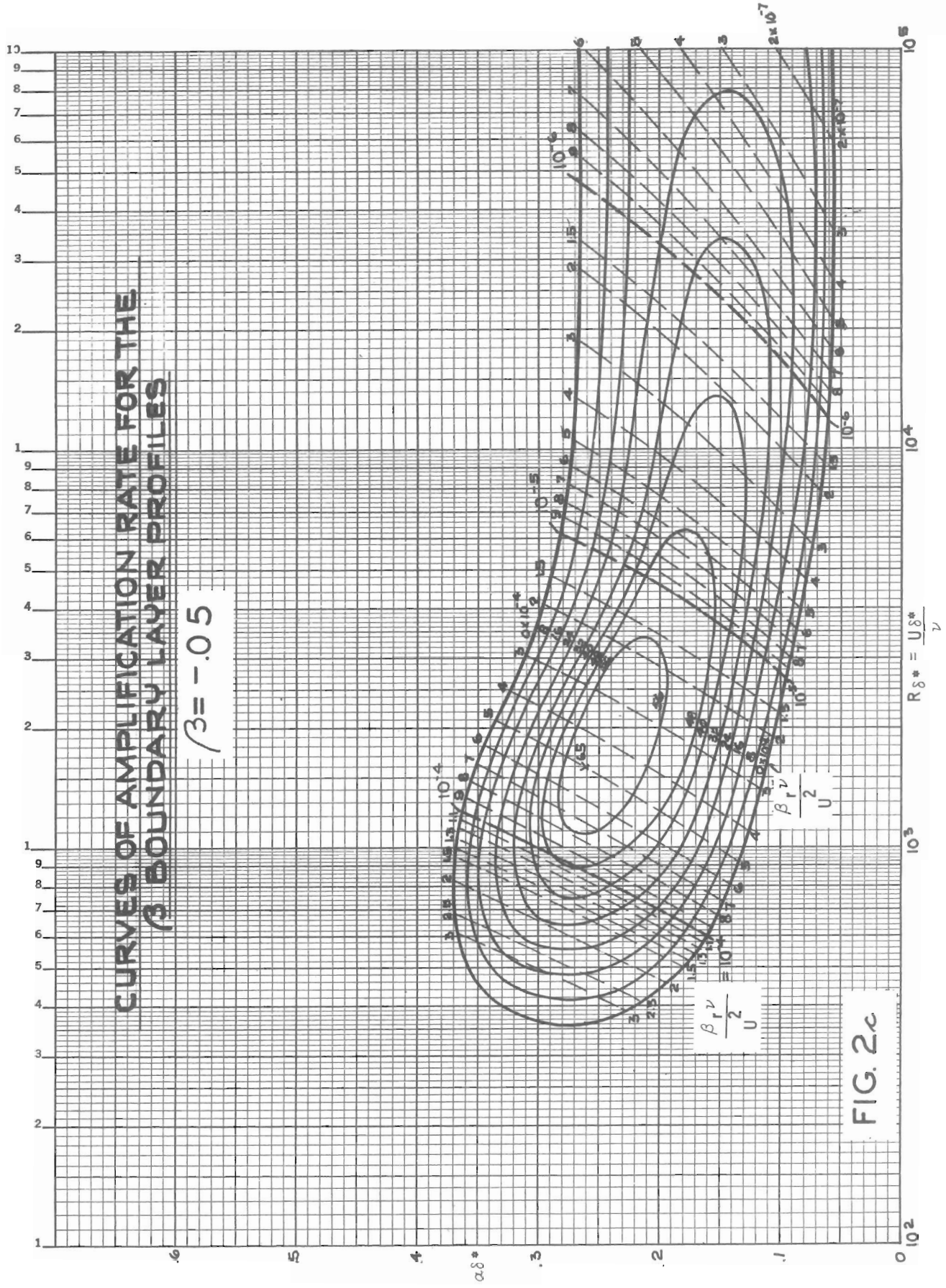
CURVES OF AMPLIFICATION RATE FOR THE
β BOUNDARY LAYER PROFILES
β = -.05
$R_{\delta^*} = \frac{U\delta^*}{\nu}$
$\alpha\delta^*$
$\frac{\beta_r \nu}{2U}$
$\frac{\beta_r \nu}{2U}$

FIG. 2c

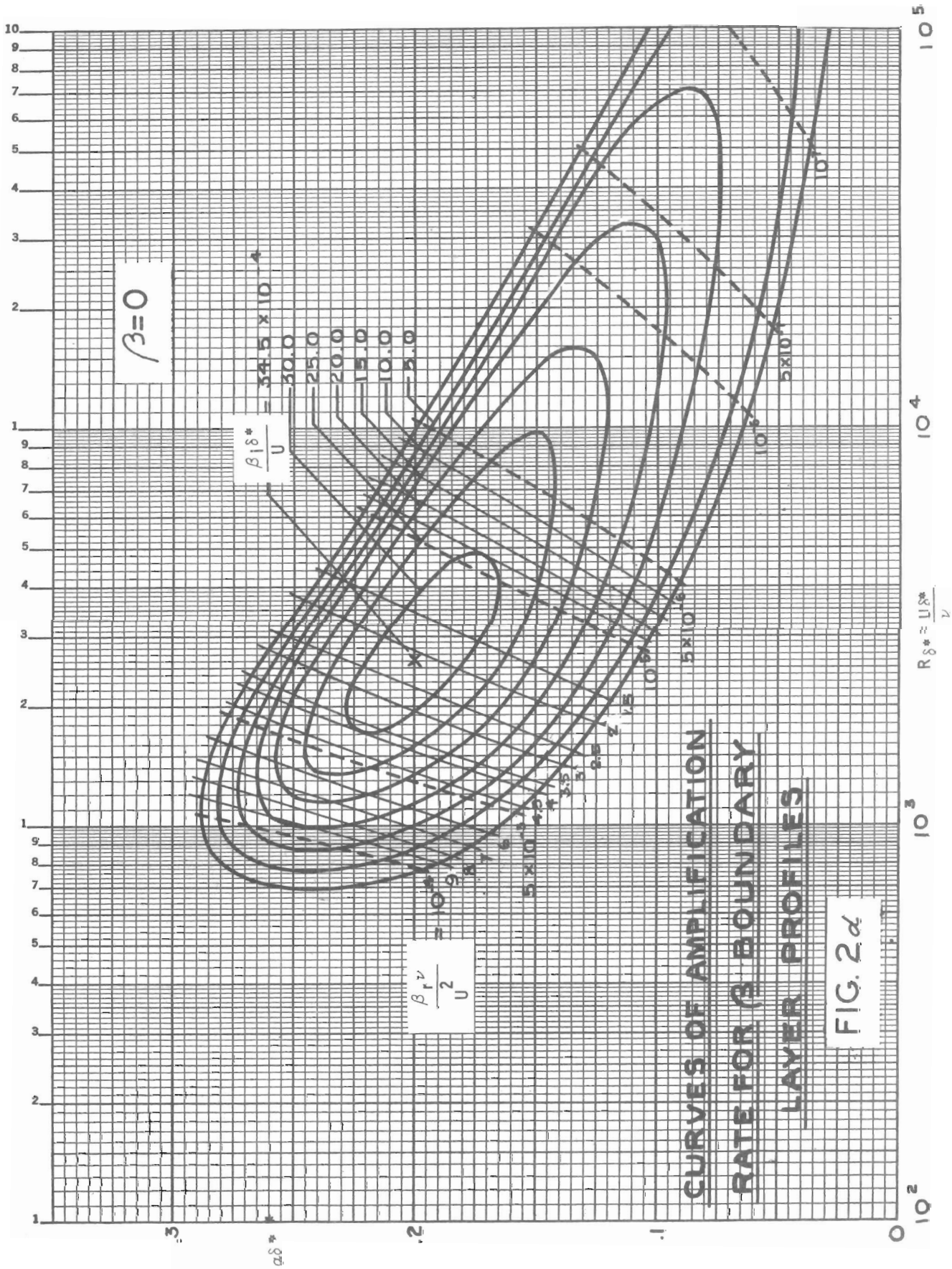
β=0
$\frac{\beta_1 \delta^*}{U}$ = 34.5 x 10⁻⁴
30.0
25.0
20.0
15.0
10.0
5.0
$\frac{\beta_r \nu}{U^2}$ = 0.9 x 10⁻⁶
5 x 10⁻⁶
10⁻⁵
5x10⁻⁵
10⁻⁴
5x10⁻⁴
10⁻³
$R_{\delta^*} = \frac{U\delta^*}{\nu}$
$\alpha\delta^*$
CURVES OF AMPLIFICATION RATE FOR G BOUNDARY LAYER PROFILES
FIG. 2d

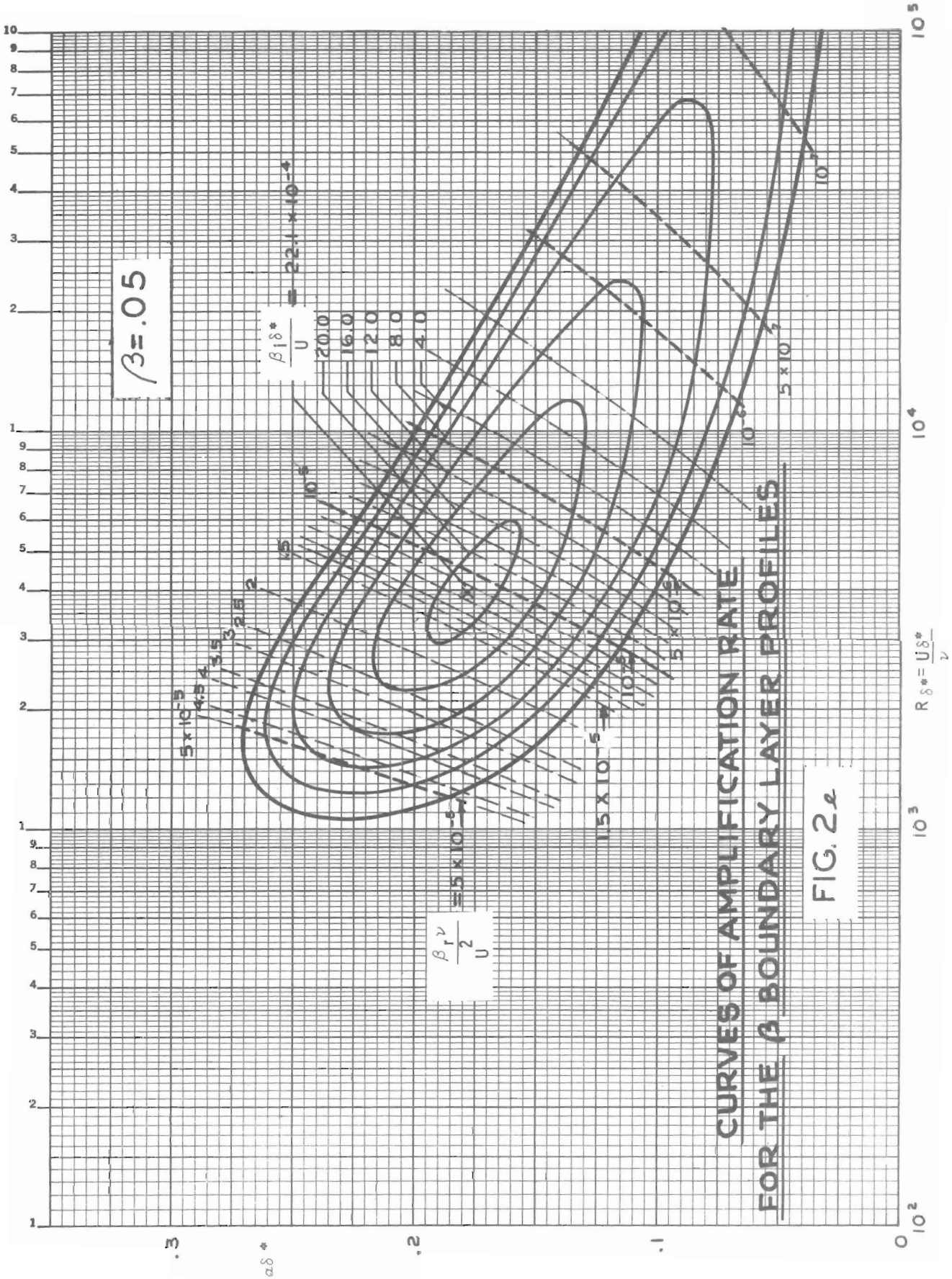
β=.05
$\frac{\beta_1 \delta^*}{U}$ = 22.4 × 10⁻⁴
20.0
16.0
12.0
8.0
4.0
5 × 10⁻⁵
4.5
4.0
3.5
3.0
2.5
2
1.5
1.0
.5
$\frac{\beta_r \nu}{2U}$ = 5 × 10⁻⁶
1.5 × 10⁻⁵
5 × 10⁻⁵
10⁻⁴
2 × 10⁻⁴
5 × 10⁻⁴
10⁻³
$R_{\delta^*} = \frac{U\delta^*}{\nu}$
$\alpha\delta^*$
CURVES OF AMPLIFICATION RATE
FOR THE β BOUNDARY LAYER PROFILES
FIG. 2a

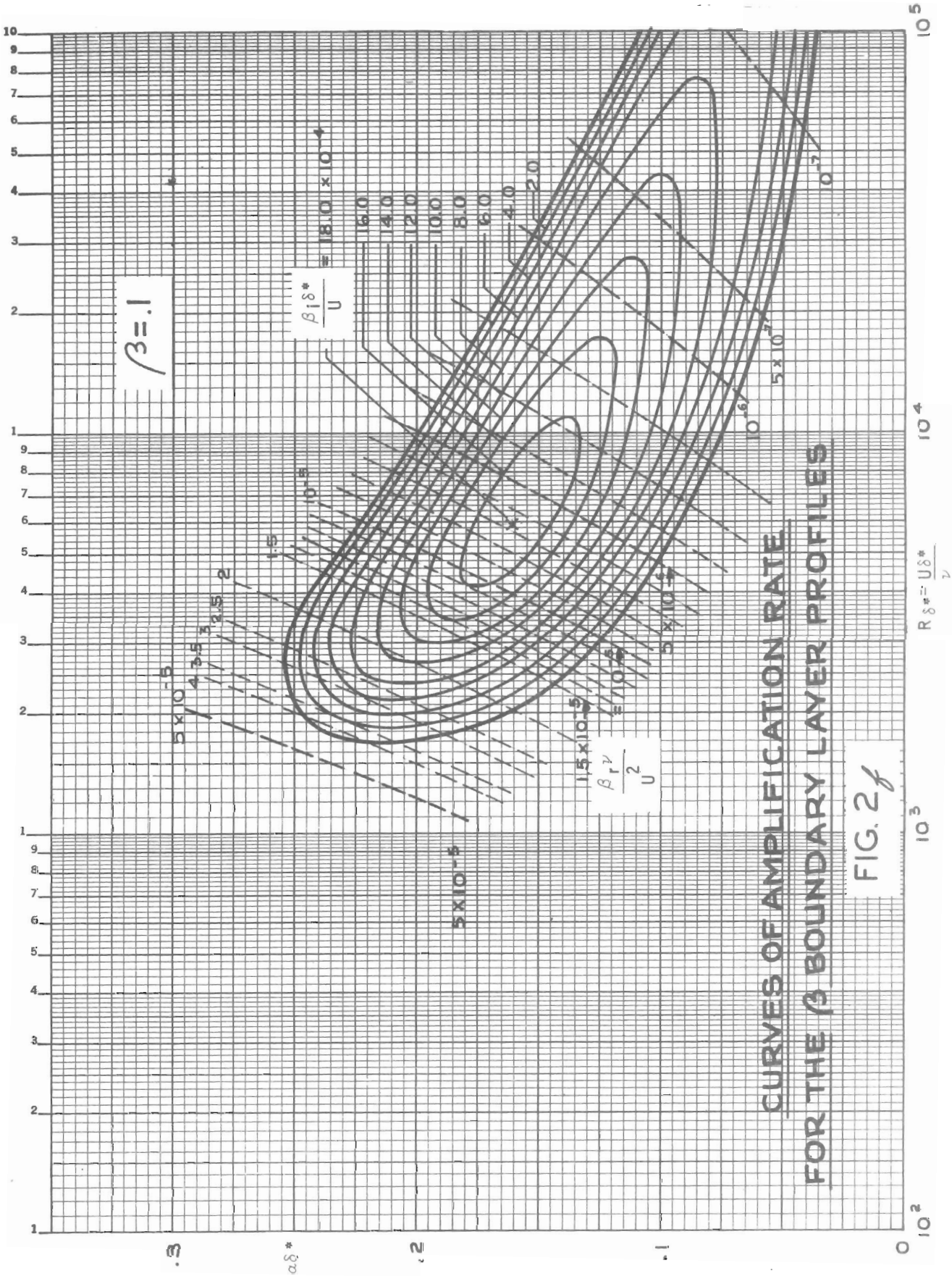
β=.1
$\frac{\beta_i \delta^*}{U}$ = 18.0 x 10⁻⁴
16.0
14.0
12.0
10.0
8.0
6.0
4.0
2.0
10⁻⁶
5x10⁻⁶
10⁻⁵
1.5x10⁻⁵
$\frac{\beta_r \nu}{U^2}$
5x10⁻⁵
10⁻⁴
5x10⁻⁴
10⁻³
5x10⁻³
10⁻²
5x10⁻²
10⁻¹
5x10⁻¹
$\alpha\delta^*$
$R_{\delta^*} = \frac{U\delta^*}{\nu}$
CURVES OF AMPLIFICATION RATE
FOR THE β BOUNDARY LAYER PROFILES
FIG. 2f

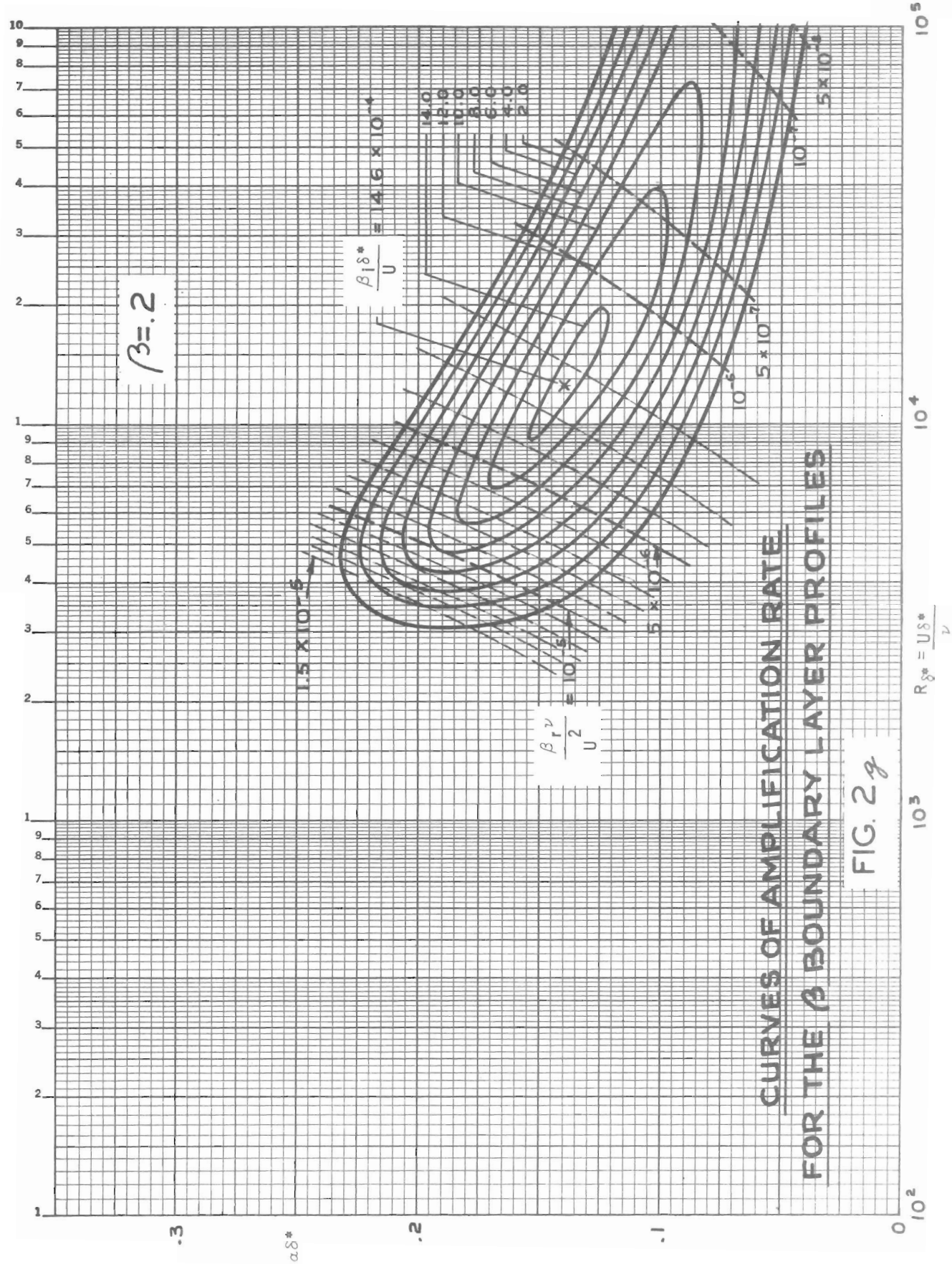
β=.2
$\frac{\beta_i \delta^*}{U} = 14.6 \times 10^{-4}$
$\frac{\beta_r \nu}{U^2} = 10^{-6}$
1.5×10^{-6}
5×10^{-6}
10^{-5}
5×10^{-5}
10^{-4}
5×10^{-4}
14.0
12.0
10.0
8.0
6.0
4.0
2.0
$\alpha\delta^*$
$R_{\delta^*} = \frac{U\delta^*}{\nu}$
CURVES OF AMPLIFICATION RATE
FOR THE β BOUNDARY LAYER PROFILES
FIG. 2g

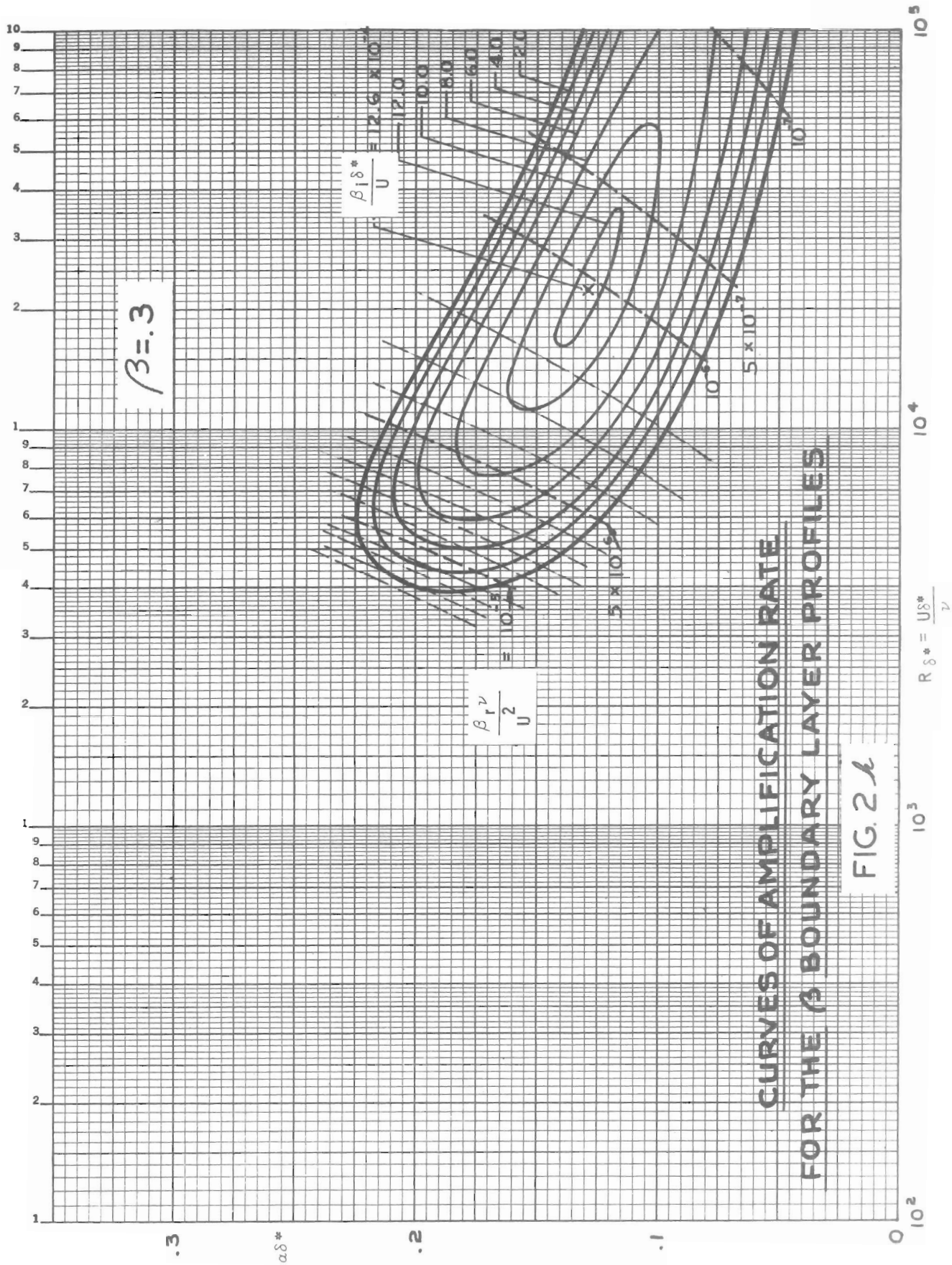
β=.3
$\frac{\beta_i \delta^*}{U}$ = 12.6 x 10⁻⁴
12.0
10.0
8.0
6.0
4.0
2.0
$\frac{\beta_r \nu}{U^2}$ = 10⁻⁵
5 x 10⁻⁶
10⁻⁶
5 x 10⁻⁷
10⁻⁷
$R_{\delta^*} = \frac{U\delta^*}{\nu}$
$\alpha\delta^*$
CURVES OF AMPLIFICATION RATE
FOR THE (3 BOUNDARY LAYER PROFILES

FIG. 24

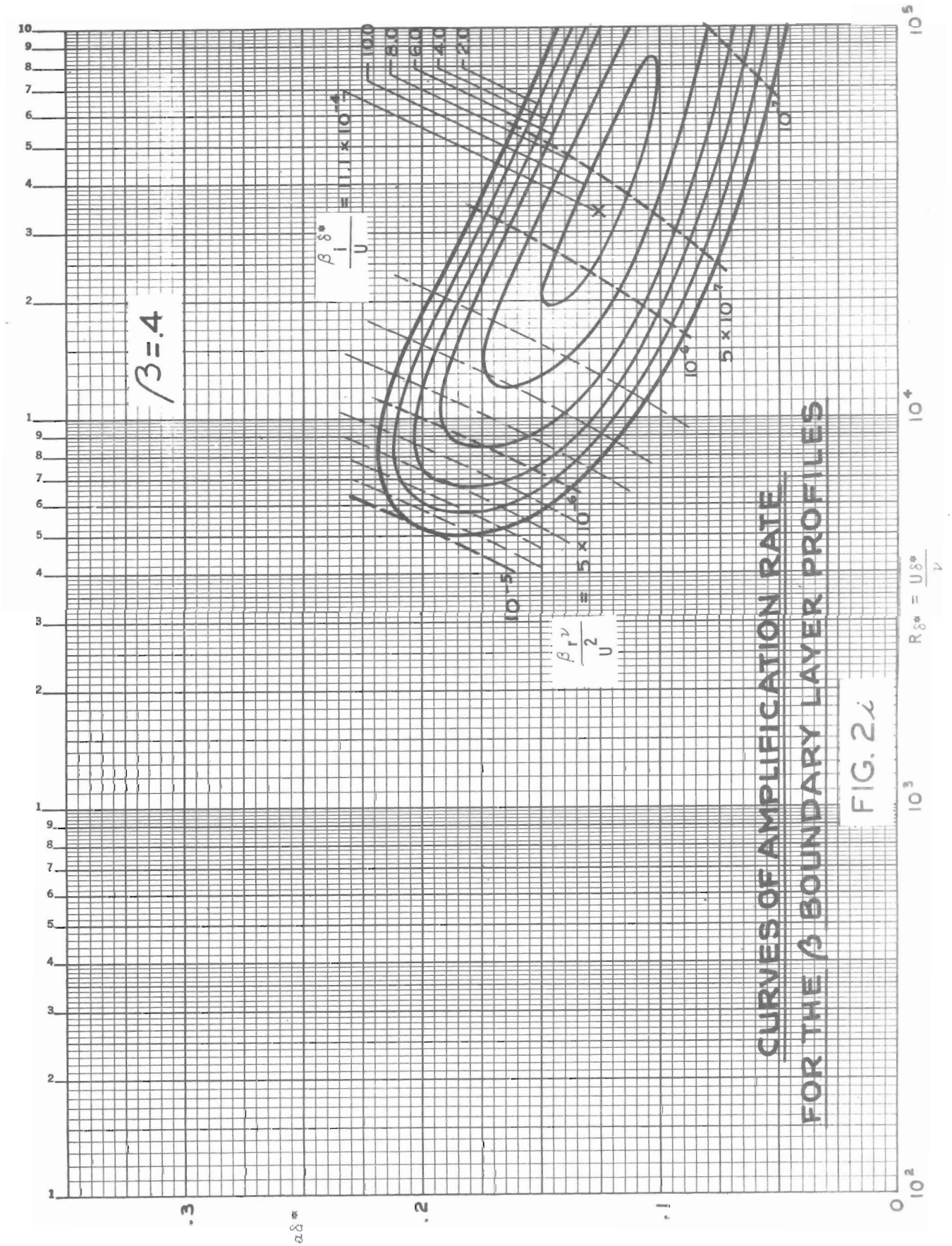
β = .4
CURVES OF AMPLIFICATION RATE
FOR THE β BOUNDARY LAYER PROFILES
FIG. 2i
$\frac{\beta_r \nu}{U^2}$ = 5 x 10⁻⁵
$\frac{\beta_i \delta^*}{U}$ = 1.1 x 10⁻⁴
$R_{\delta^*} = \frac{U\delta^*}{\nu}$
$\alpha\delta^*$

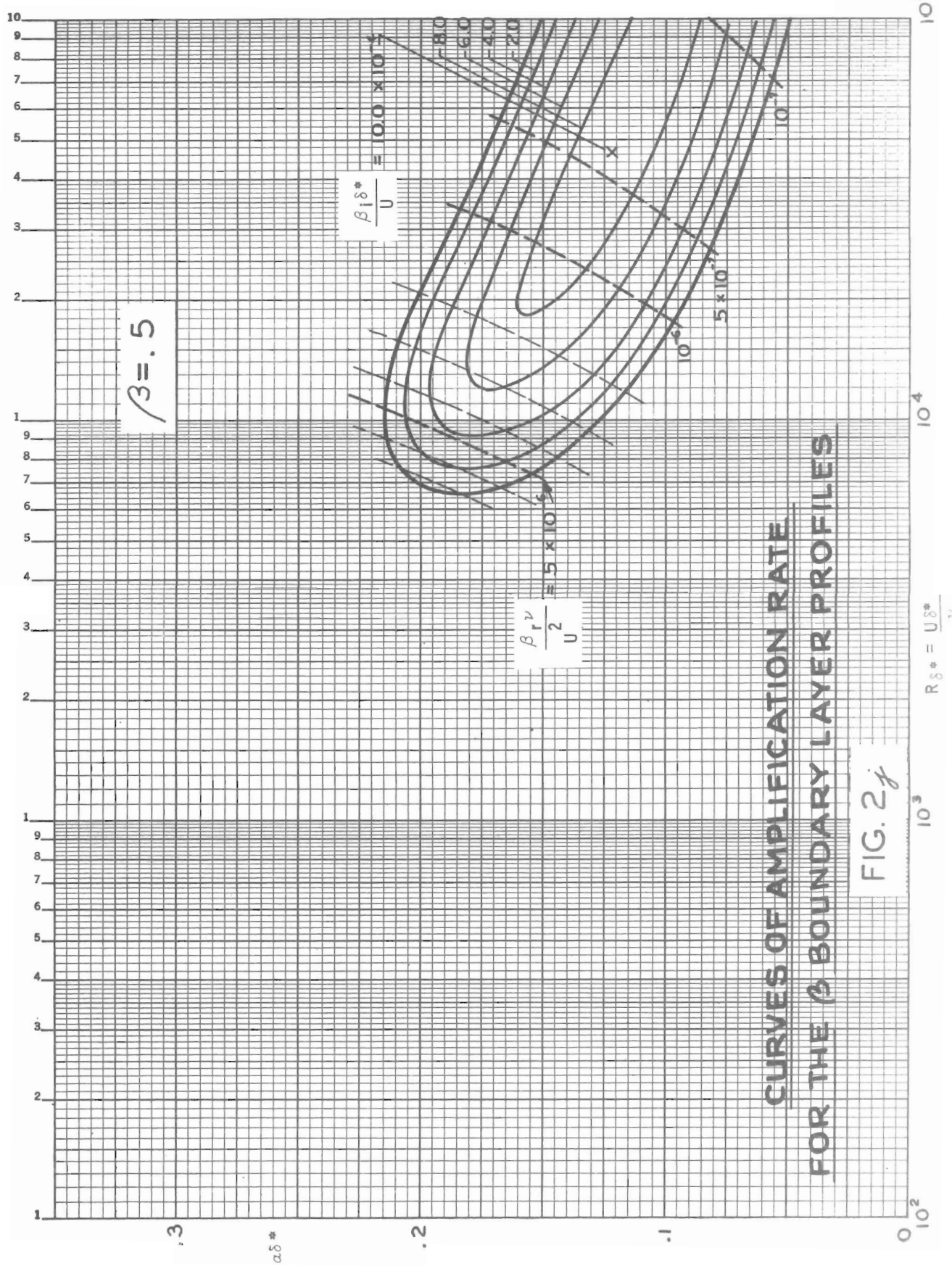

CURVES OF AMPLIFICATION RATE FOR THE δ BOUNDARY LAYER PROFILES

FIG. 2f

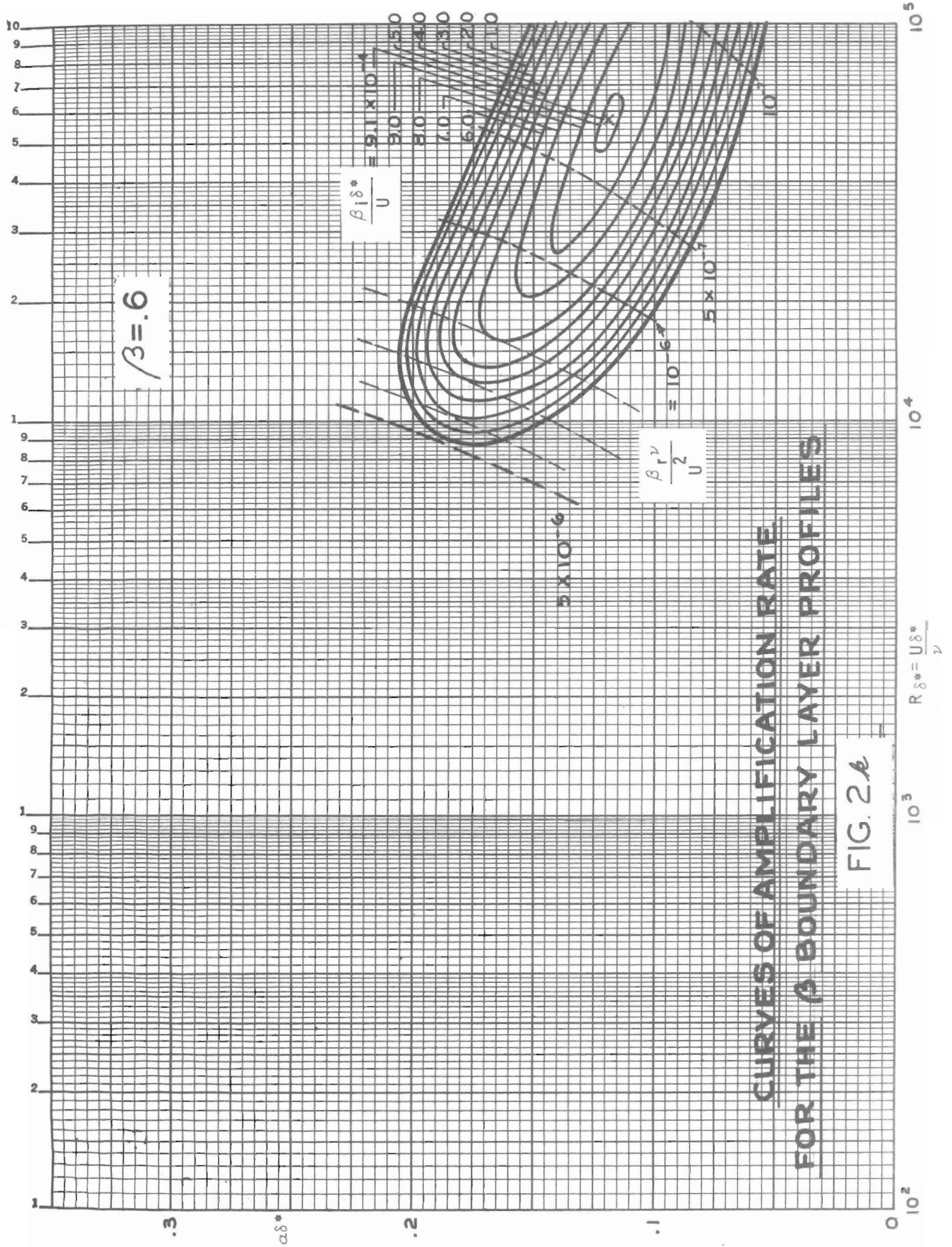
β=.6
$\frac{\beta_i \delta^*}{U} = 9.1 \times 10^{-4}$
$\frac{\beta_r \nu}{U^2} = 10^{-6}$
5×10^{-6}
5×10^{-5}
10^{-4}
$R_{\delta^*} = \frac{U\delta^*}{\nu}$
$\alpha\delta^*$
CURVES OF AMPLIFICATION RATE
FOR THE β BOUNDARY LAYER PROFILES

FIG. 2k

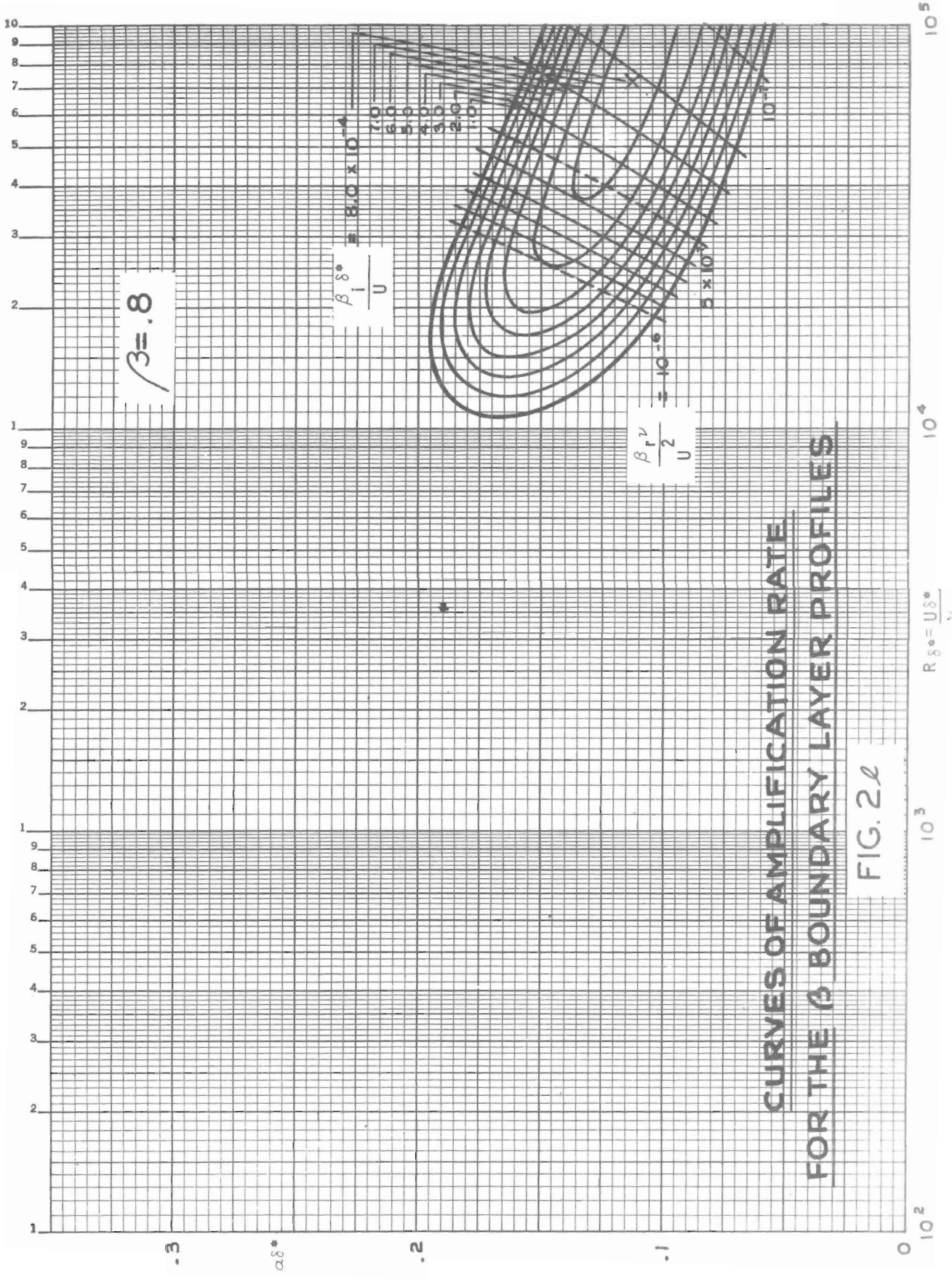

CURVES OF AMPLIFICATION RATE
FOR THE β BOUNDARY LAYER PROFILES

FIG. 2ℓ

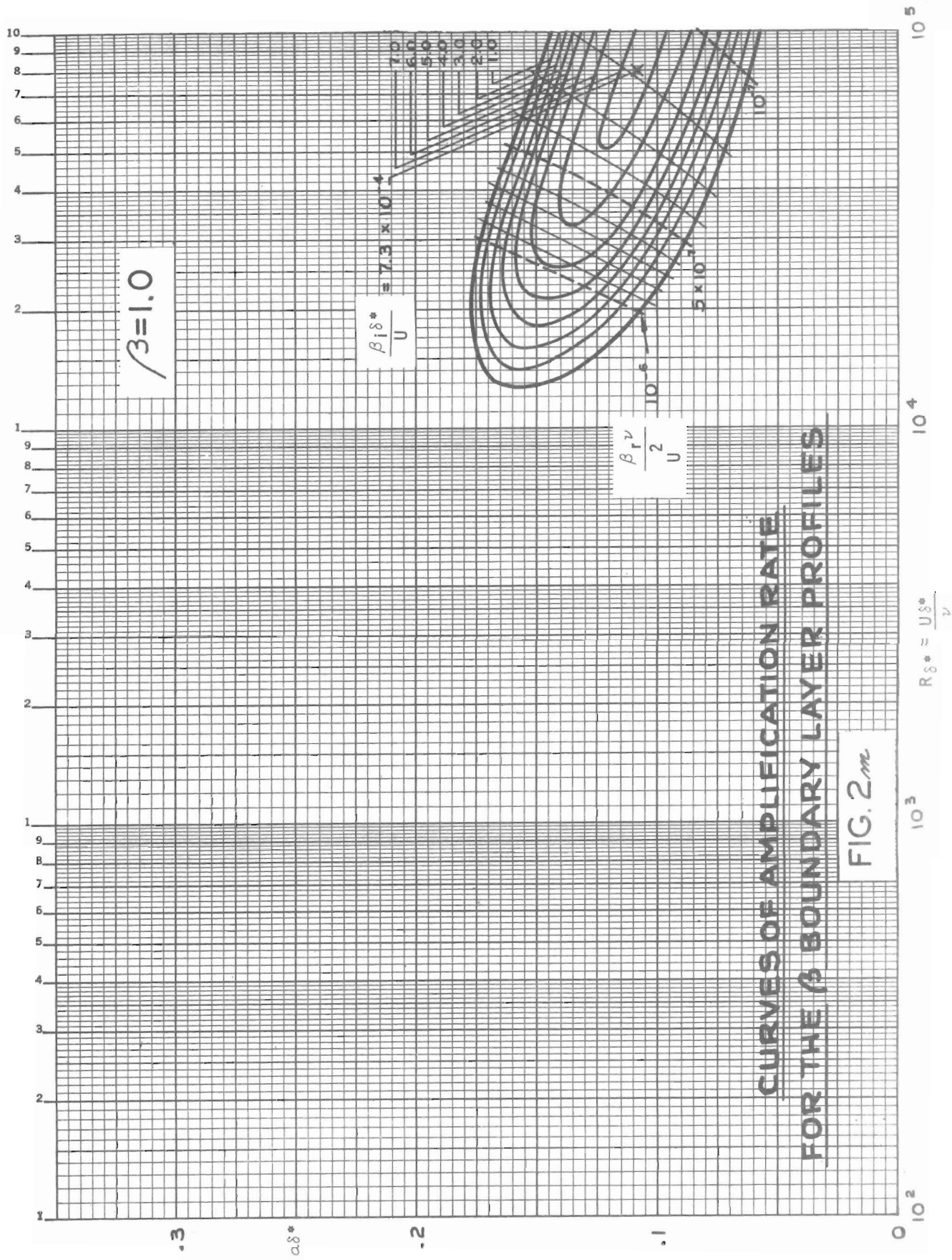

CURVES OF AMPLIFICATION RATE FOR THE β BOUNDARY LAYER PROFILES

FIG. 2m

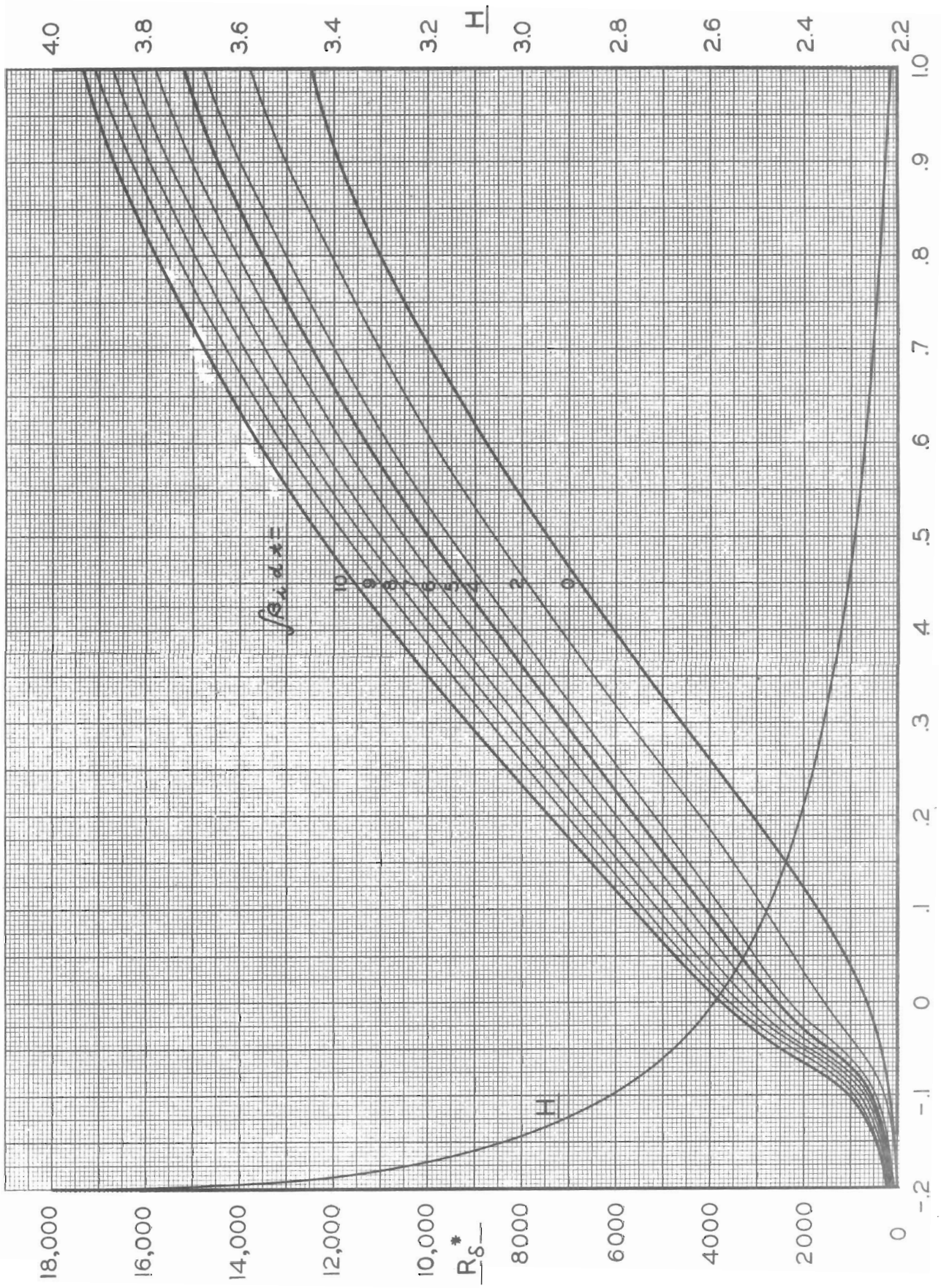

Figure 3. R_δ^* and H vs. Hartree's β for several values of the amplification ratio, constant - β flows.

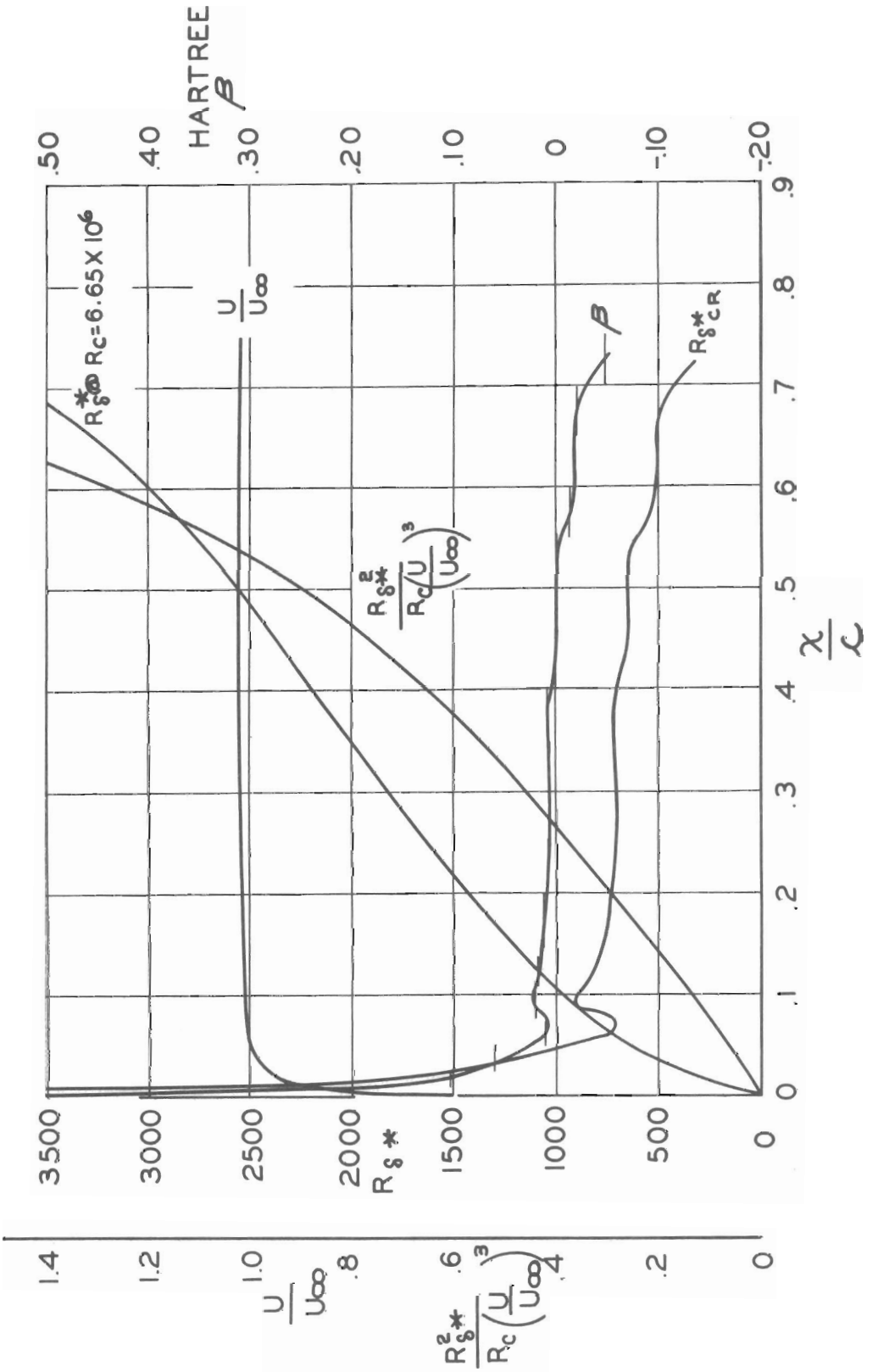

Figure 4. Boundary-layer properties, N.A.C.A. body of revolution of fineness ratio 9.0.

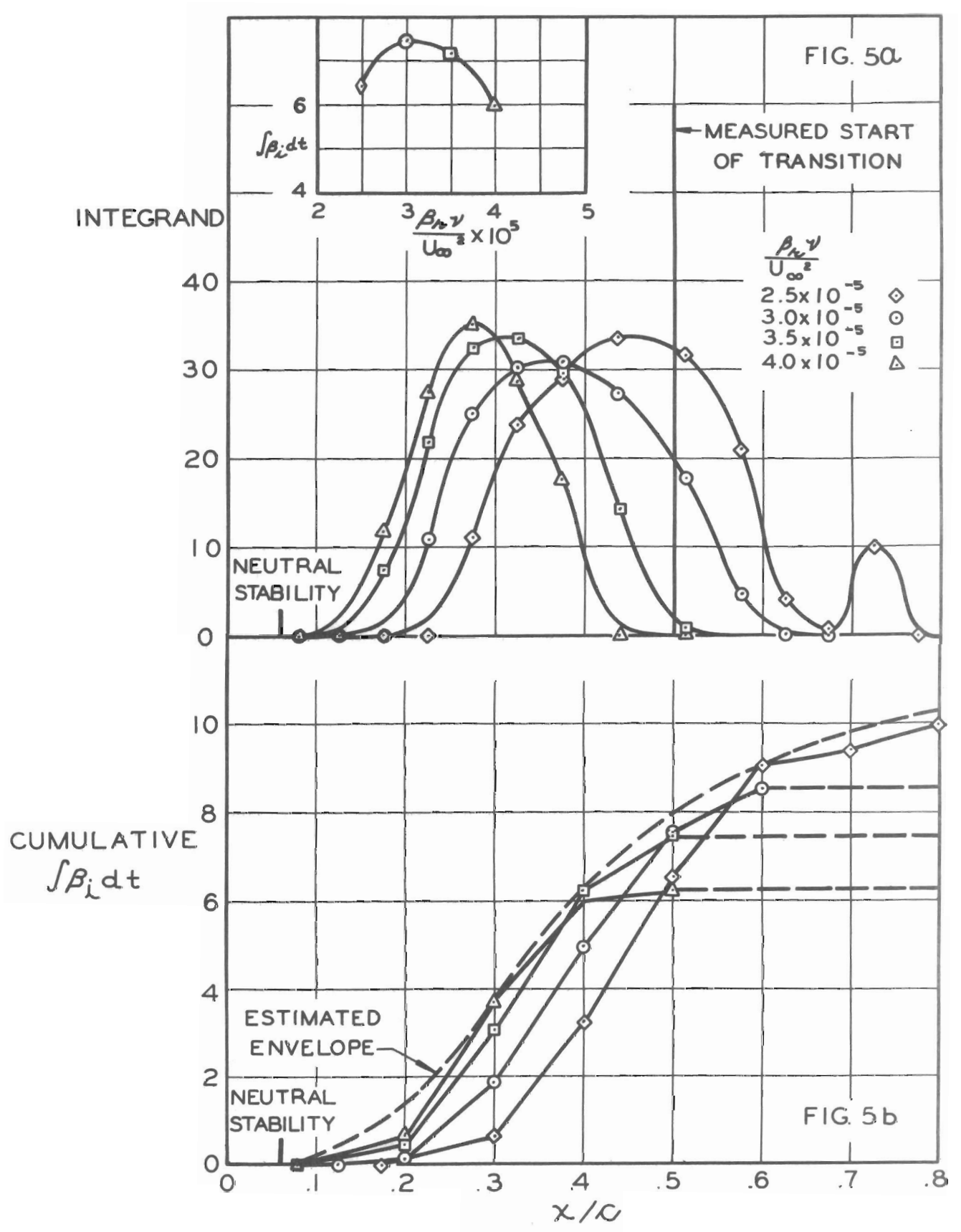

Figure 5. Growth of Tollmien-Schlichting waves at $R_c = 6.65 \times 10^6$, N.A.C.A. body of revolution of fineness ratio 9.0.

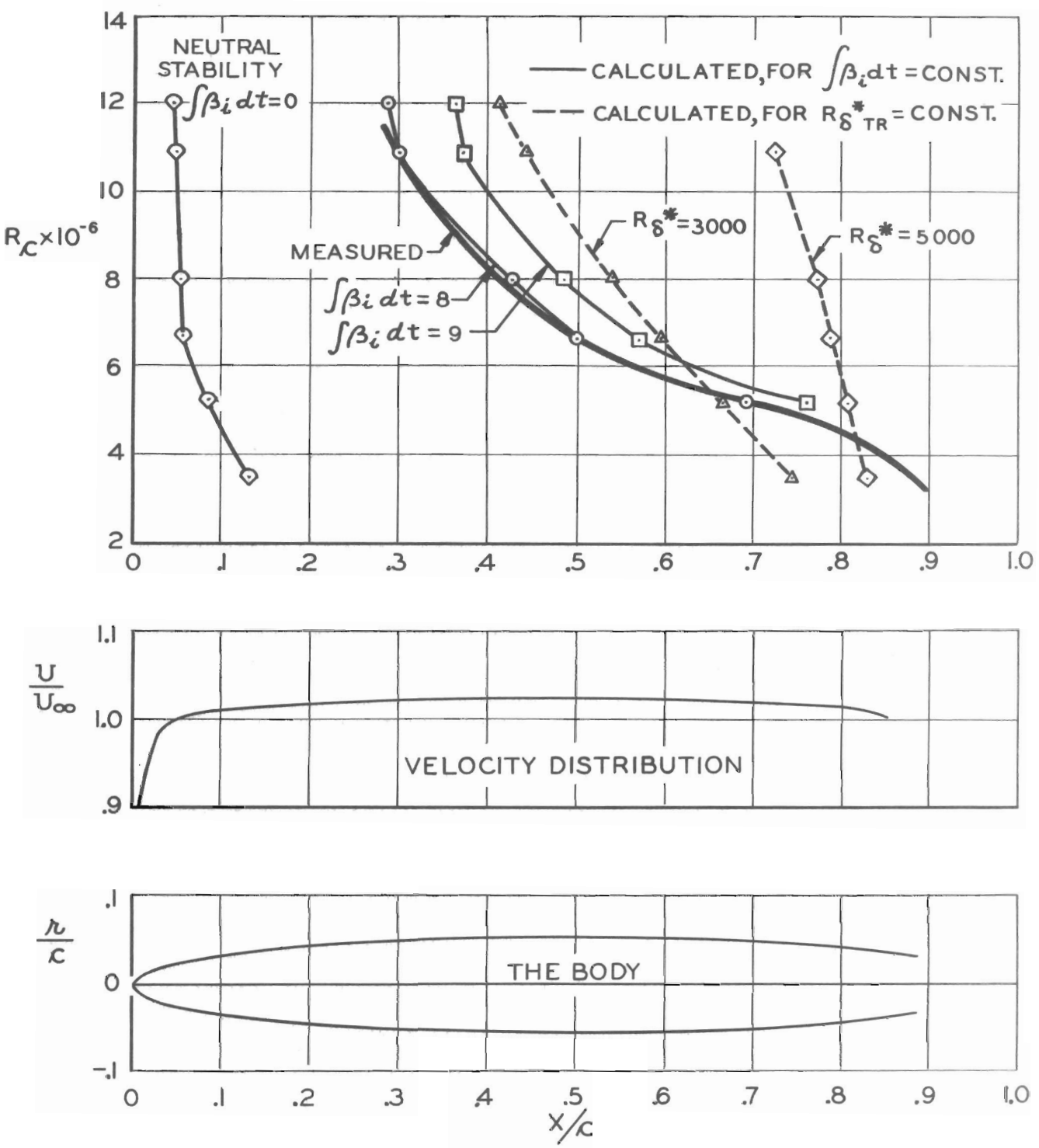

Figure 6. Comparison of two methods for estimating transition; N.A.C.A. body of revolution of fineness ratio 9.0.

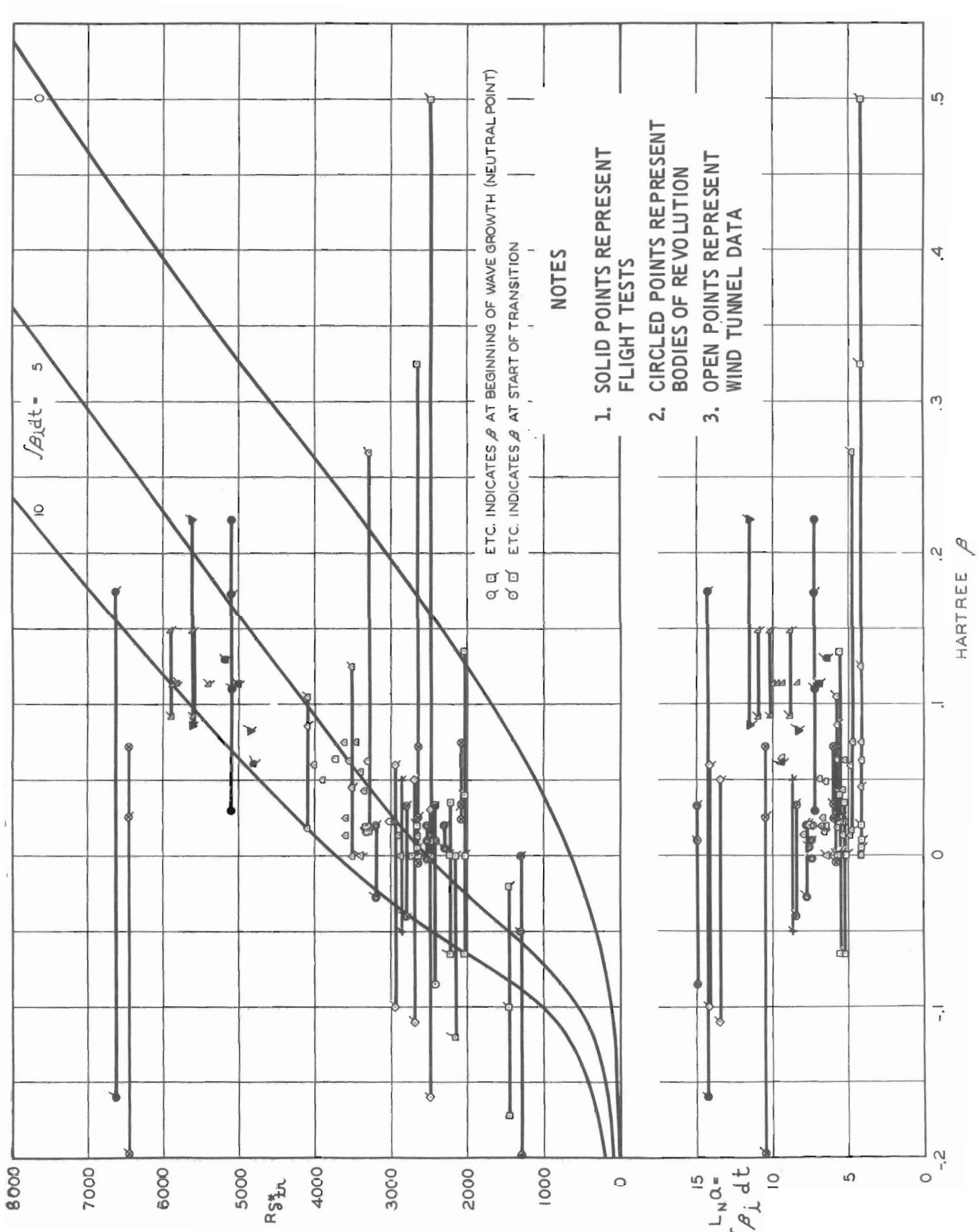

Figure 7. Calculated values of R_{δ^*} and $\int \beta_i dt$ at the start of transition. Summary of all cases analyzed. See Table I for symbols.

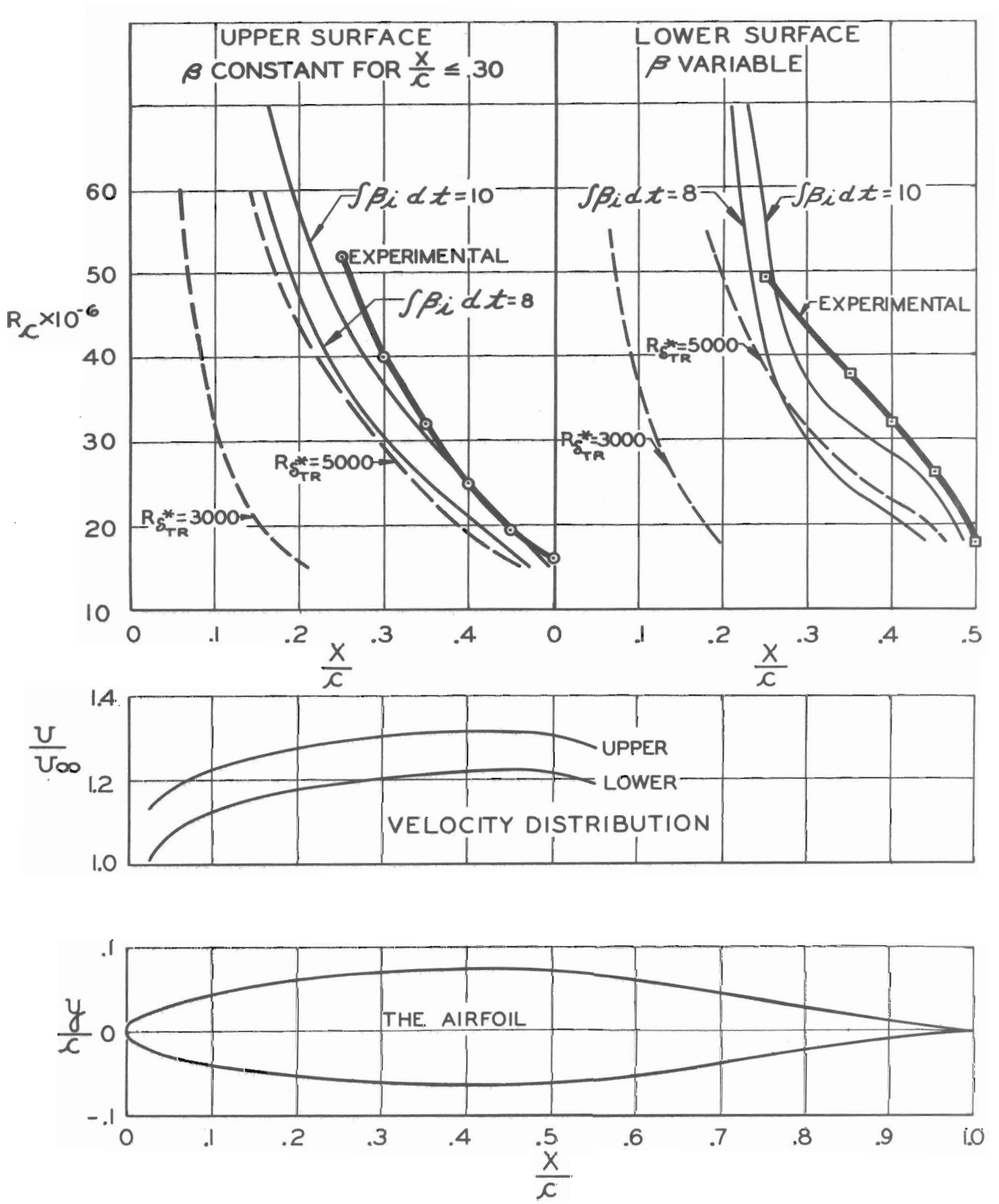

Figure 8. N.A.C.A. $65_{(215)}$ -114 Airfoil; Experimental and calculated transition curves, $C_L = 0.14$.

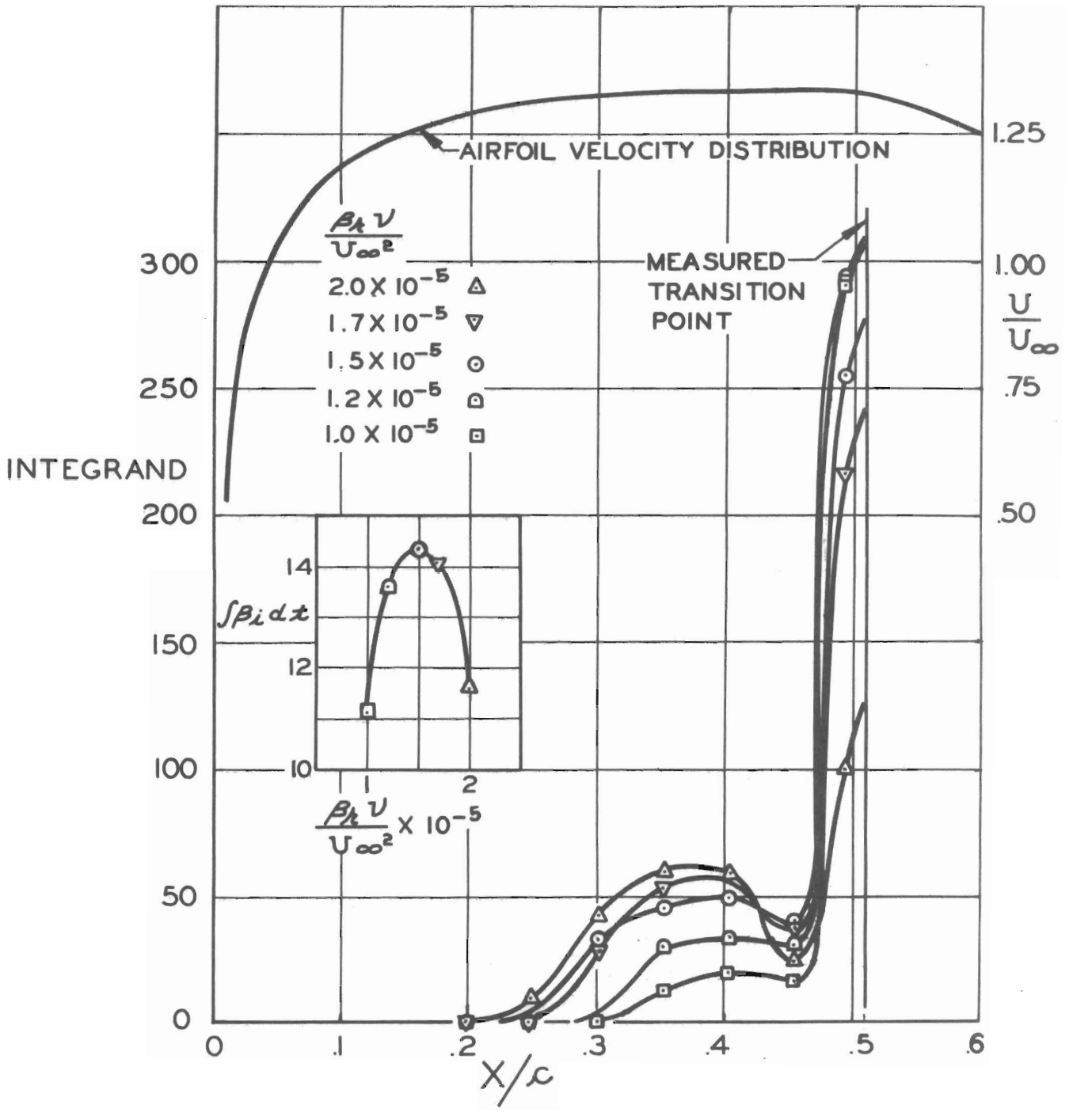

Figure 9. Computed growth of Tollmien-Schlichting waves on upper surface of HURRICANE experimental wing. $R_C = 16.35 \times 10^6$, $C_L = 0.14$.

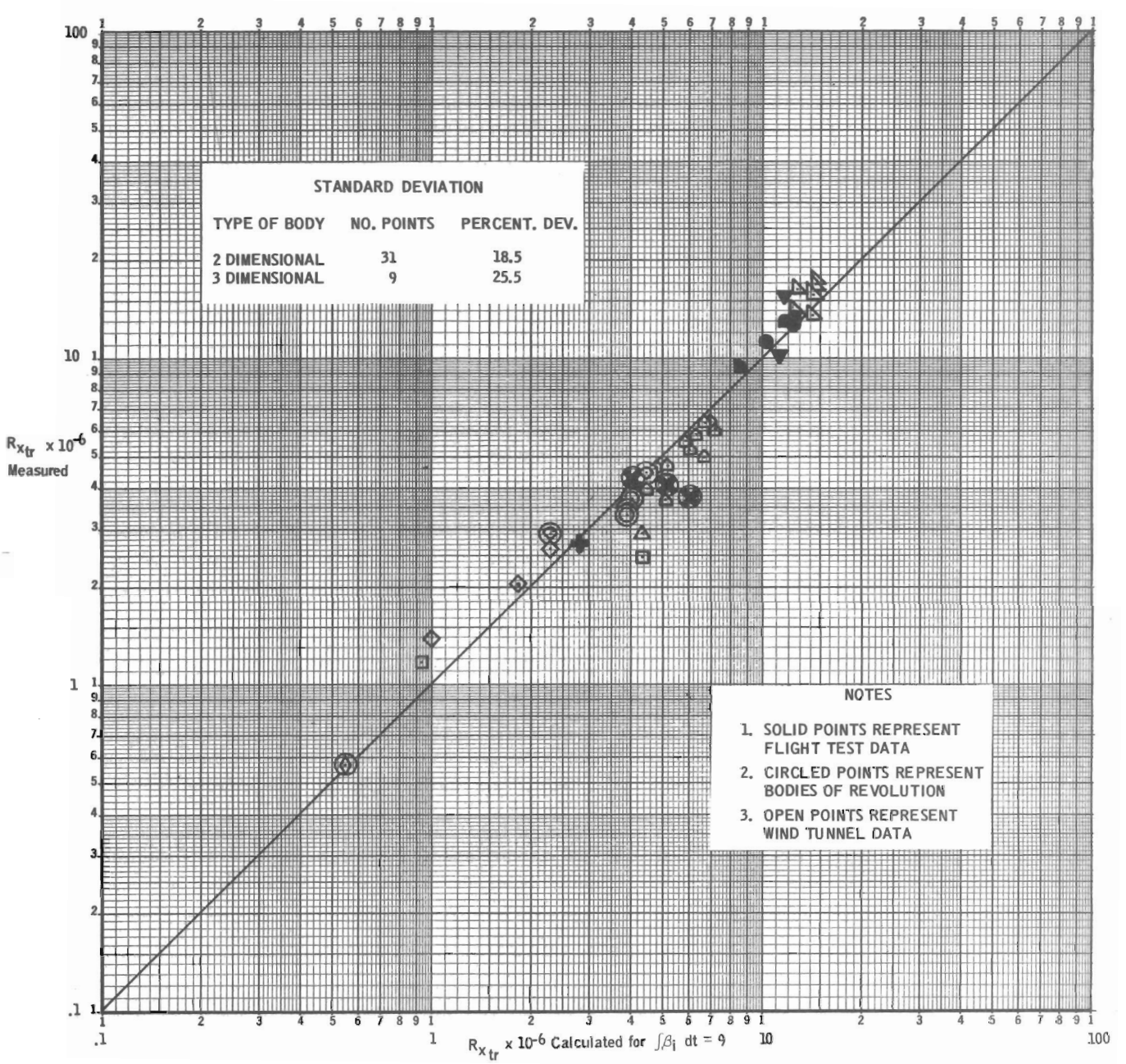

Figure 10. Transition computation--correlation between measurement and prediction by stability theory. See Table I for symbols.

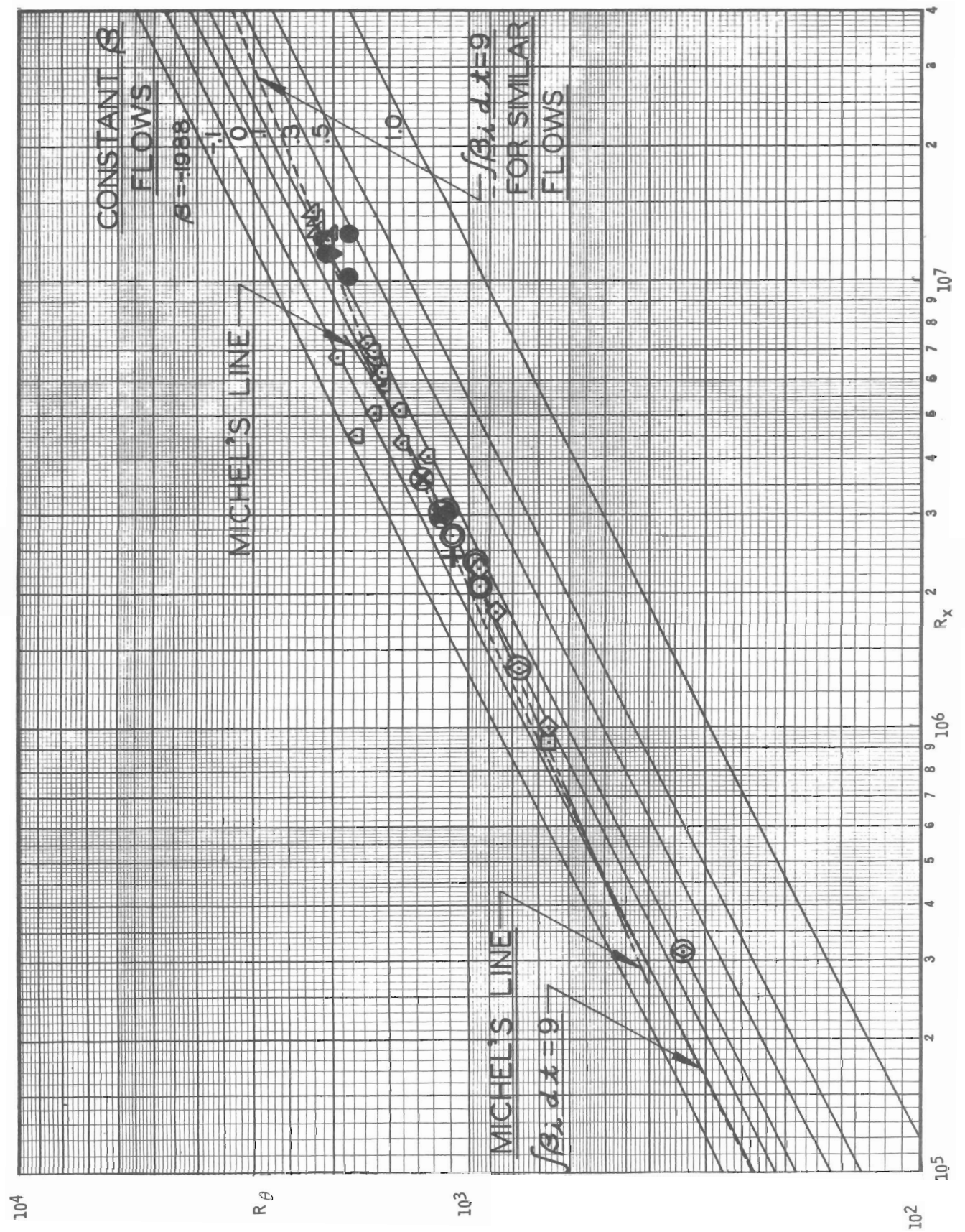

Figure 11. Locus of points corresponding to $\int \beta_i \, dt = 9$ for both similar flows and the flows of Table I. Shown also are lines of constant β for the similar flows. See Table I for symbols.

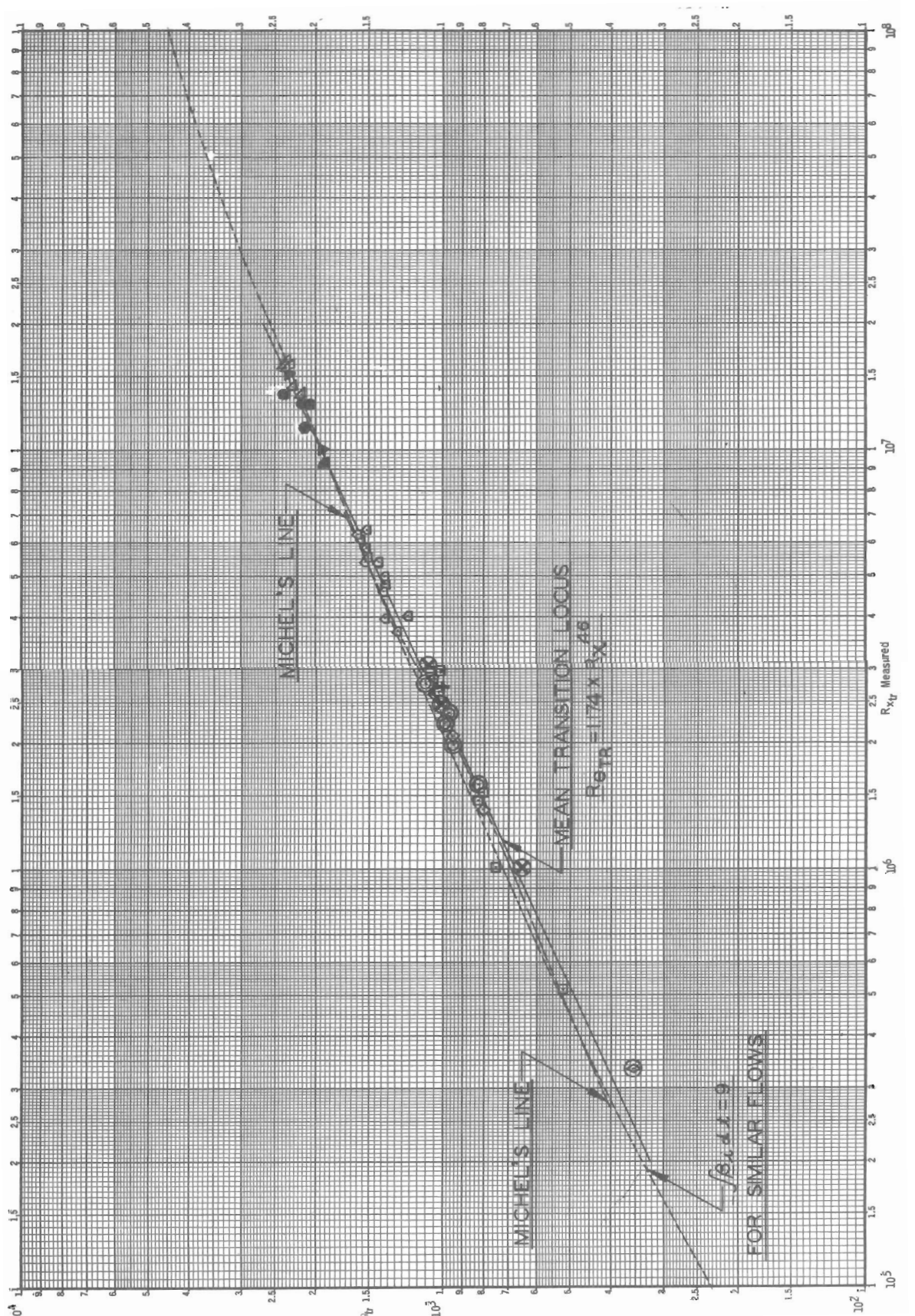

Figure 12. Summary of experimental transition data, $R_{\theta_{tr}}$ - $R_{x_{tr}}$ plot. See Table I for symbols.

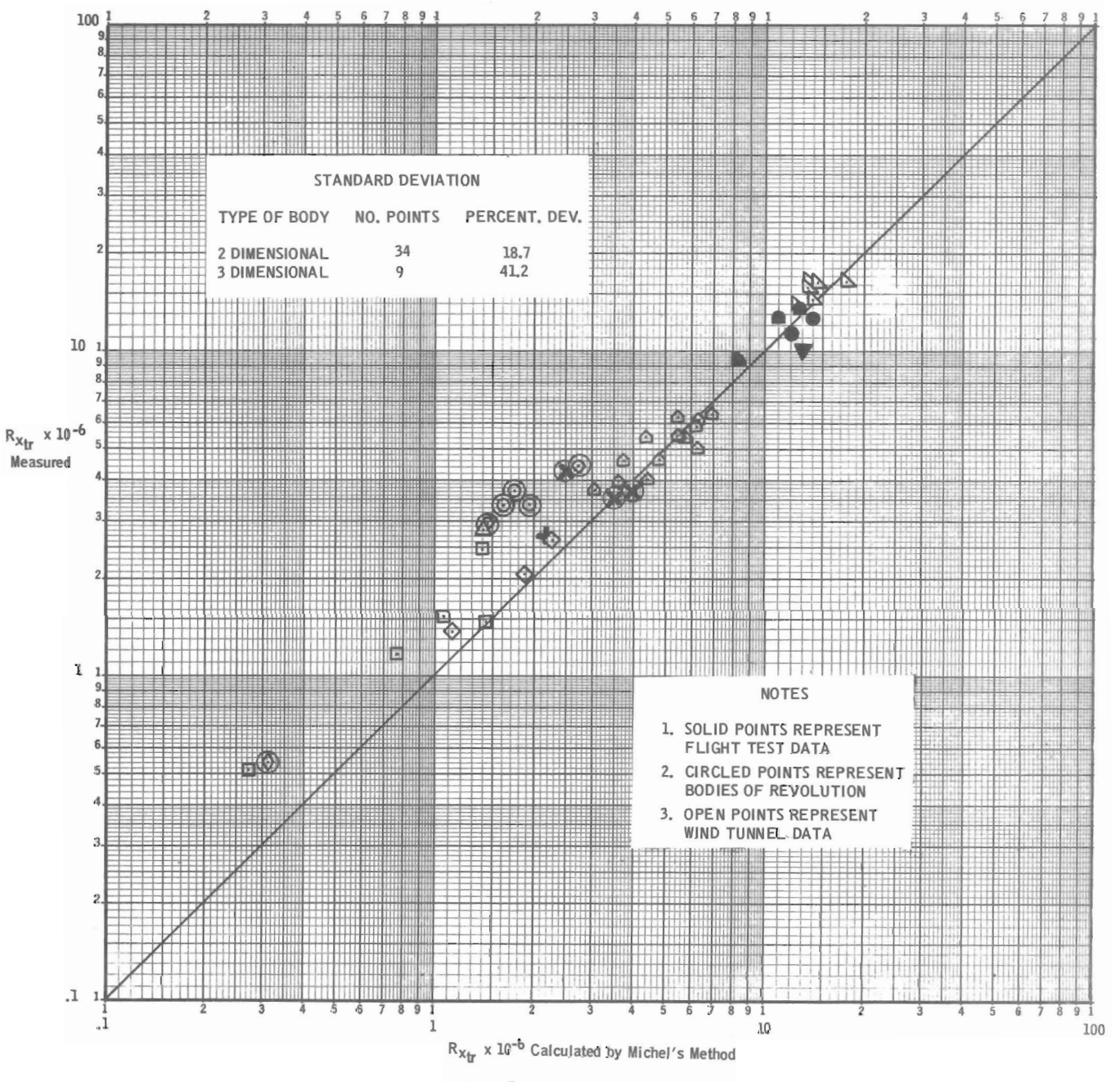

Figure 13. Transition computation--correlation between measurement and prediction by Michel's method, using Eq. 5. See Table I for symbols.